Conceptual Design of a Circulating Fluidized Bed Reactor as a Thermochemical Thermal Energy Storage System for Applications in Concentrated Solar Thermal Power Plants

ABDULLAH F. ALAJMI

A thesis
submitted as a partial fulfillment of the
requirements of the degree of

MASTER OF SCIENCE

University of Washington
2016

Committee:
John Kramlich
Philip Malte
Alberto Aliseda

Program Authorized to Offer Degree:
Mechanical Engineering

University of Washington

Abstract

Conceptual Design of a Circulating Fluidized Bed Reactor as a Thermochemical Thermal Energy Storage System for Applications in Concentrated Solar Thermal Power Plants

Abdullah F. Alajmi

Chair of the Supervisory Committee:

Professor John Kramlich

Mechanical Engineering

The use of fossil fuels as an energy resource results in both the introduction of long-life infrared-active gases into the atmosphere, and in the depletion of a finite energy resource. Neither of these results make the fossil energy option desirable in the long term. Clean renewable energy sources provide one means of avoiding these problems. Many renewable energy resources, however, suffer from the problem of varying in power during diurnal and annual cycles. Solar energy suffers from both predictable variations (e.g., the daily solar cycle) and unpredictable variations (e.g., cloud cover). This problem can be addressed by any of several proposed energy storage options. In the present work, we develop a thermochemical storage concept

where a reversible $Ca(OH)_2/CaO$ reaction is used to store energy. The system is integrated with a central receiver tower solar power plant using two circulating fluidized bed reactors. One reactor is used for an energy absorption process during the day, where the excess energy is used to drive the endothermic $Ca(OH)_2$ to CaO reaction. The other releases energy during the night using the reverse exothermic reaction. The energy absorbing reactor is placed in the tower where it receives heat reflected from the heliostat field where extended surfaces (fins) are used to improve heat flow into the fluidized bed. The energy discharging reactor is insulated using refractory with heat being absorbed by water/steam flowing inside water-walls that are in contact with the fluidized bed material. Conceptual design work suggests that one reactor will have a 7.2 m diameter and a the other will have a 8 m diameter, with a height of 37.5 m for both. It is estimated that the levelized cost of electricity (LCOE) will be 19 cents/kWh, which is higher than LCOE of a concentrated solar power (CSP) plant with no storage system, however, electricity with the thermochemical thermal energy storage (TES) system will be produced consistently for 24 hours overcoming the intermittency problem of renewable energy source.

Acknowledgment

I am highly indebted in the preparation of this thesis to several people for their extended help, which without their help the completion of this thesis would not have been possible. First of all is my advisor Professor John Kramlich for providing me with the unique opportunity to work in this research area and for his encouragement, mentorship and guidance at all levels. His efforts and help will always be appreciated. Also, I would like to express my deepest gratitude to my parents and siblings for their everlasting help, encouragement and patience through good days and bad days.

Financial support provided from Kuwait University and the Ministry of Higher Education in Kuwait is greatly acknowledged.

Table of Contents

List of Tables

List of Figures

Chapter 1: Background

1.1 Introduction

Energy usage is increasing across the globe, both due to the increase in population and the increase in per capita energy use. While conservation has reduced per capita demand in the developed world, this is more than offset by increases in the standard of living in the developing world. According to United Nations reports, the world population has surpassed seven billion human beings, and population growth continues to accelerate (UN, 2015). Moreover, according to the Energy Information Administration, 67% of the electricity produced in the United States in 2014 is from fossil fuels (EIA, 2015). Fossil fuel resources required millions of years to develop, and they are essentially non-renewable given the rate at which they are being used. If the use of these resources continues at the present rate, it is predicted that oil and natural gas resources will last for decades while coal will last for centuries (MacKay et al., 2009). In other words, these resources are ultimately finite and the sole dependence on them is not feasible in the long term. As these resources start to deplete, an energy crisis will emerge and the prices for fossil fuels will increase significantly (EIA, 2015).

A separate problem for fossil fuel based power generation is the release of infrared-active gases into the atmosphere. One of the most important global warming species is carbon dioxide. Carbon dioxide and other greenhouse gasses (GHG) like methane have the ability to trap heat from leaving the Earth's atmosphere, which has the potential to cause catastrophic climate change within a century (Tweidell et al., 2006). Over the past 150 years, CO_2 concentrations in the atmosphere have increased by 25% because of the burning of fossil fuels (MacKay et al., 2009). Since the industrial revolution, the CO_2 concentration has increased to 400 parts per million, as shown in Figure 1 (MacKay et al., 2009). Several other gasses are produced that effect air quality like nitrous oxide, nitric oxide, sulfur oxide and hydrocarbons (MacKay et al., 2009). These gasses can lead to major health problems and can affect crops because of acid rain (MacKay et al., 2009).

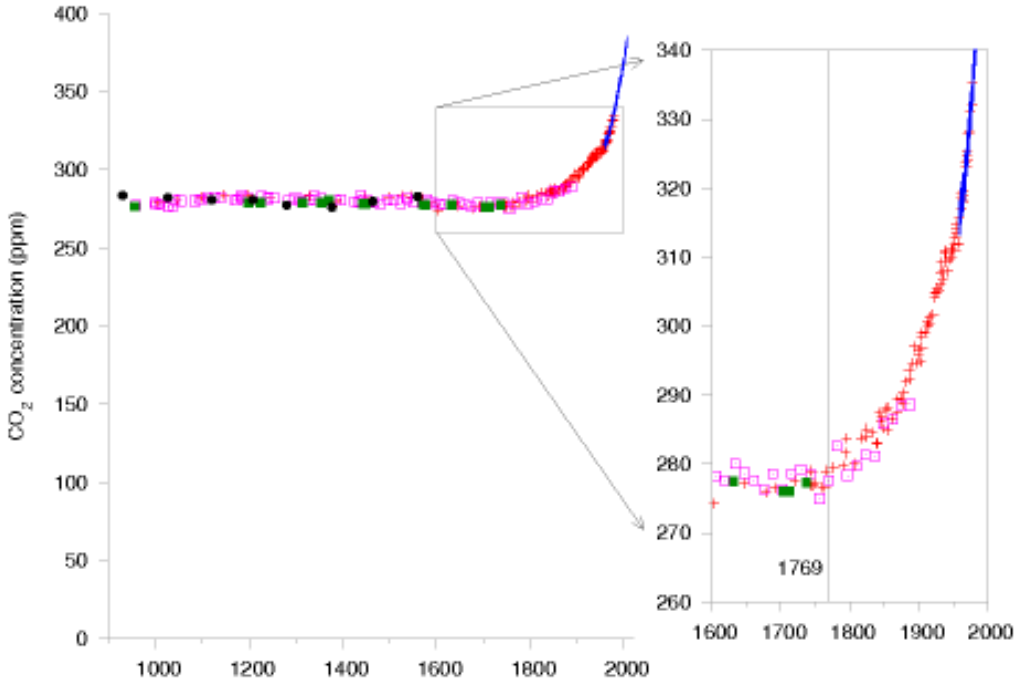

Figure 1: Atmospheric carbon dioxide concentration (MacKay et al., 2009).

Renewable energy options address both the greenhouse gas problem and the resource depletion problem. Renewable energy can be defined as "energy obtained from natural and persistent flows of energy occurring in the immediate environment" (Tweidell et al., 2006). Solar energy is an example where natural and persistent flows in a predictable way. This energy is flowing in nature regardless of whether or not a device is used to harness the flow.

1.2 Solar Energy

Solar Energy is a form of renewable energy that can be used to produce electricity in two ways: thermally in concentrated solar power (CSP) plants, or photo-electrically via photovoltaic (PV) solar cells (Tweidell et al., 2006).

The majority of solar radiation reaches the Earth in wavelengths between 0.3 and 2.5 μm, which includes infrared, visible light and ultraviolet waves (MacKay et al., 2009). The maximum solar radiation flux reaching the Earth's surface is about 1000 W/m^2 (MacKay et al., 2009). Solar energy is generated only in the presence of the sun, which means one loses the ability to produce electricity during the night, and that production is severely curtailed on cloudy days. Electricity production will

also vary across the year. For example, the solar intensity in the northern hemisphere reaches a peak during June and July and is at a minimum during December and January (Tweidell et al., 2006). Therefore, this non-consistency in the production from day to night, from day to day, and from season to season affects the reliability of renewable energy power plants. One possible solution for this problem is through the use of thermal energy storage (TES) systems.

1.3 Types of Solar Thermal Power Plants

Solar thermal power plants can operate two modes. In the first, the solar energy is used to directly heat the water/steam working fluid. In the second, the solar energy is used to heat an intermediate fluid (e.g., molten salt), which in turn is used to raise steam in a separate heat exchanger. The former system has the advantage of simplicity, while the latter (termed a thermal energy storage system, or TES as noted above) allows some flexibility for storing energy. TES systems can be applied to both central receiver CSP plants (solar towers), and to parabolic troughs CSP plants (Tweidell et al., 2006). Each CSP plant has the following major components (Gil et al., 2010):

- Concentrator
- Receiver
- Power block unit
- Transport/ storage Media (optional)

1.3.1 Central Receivers

As shown in the Figure 2, central receiver power plants consist of many heliostats (mirrors) concentrating the solar radiation toward a central receiver at the top of a tower. If the system does not have a TES system then water will pass through the receiver, which will act as a steam generator for a standard Rankine cycle. If the CSP plant has a TES system, a storage medium such as molten salt is heated in the tower instead of the water/steam system, and heat exchangers are used to transfer heat from the storage medium to water system (Tyner et al., 2014). Such media can save some of the heat to be used after the sunset. More details about TES systems will be provided in Section 1.4.

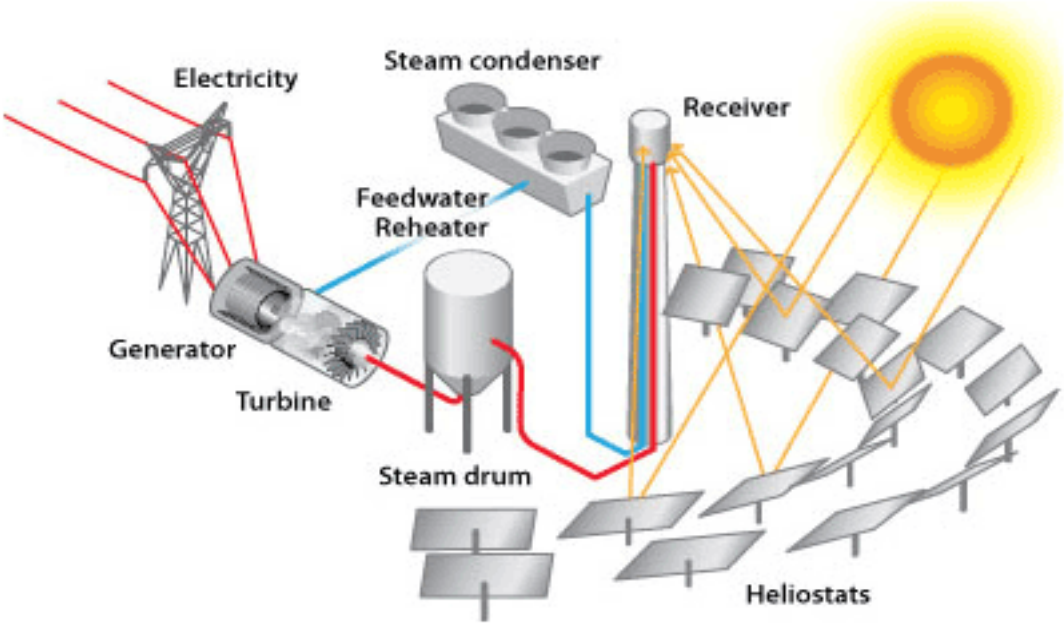

Figure 2: central receiver CSP plant (Cekirge et al., 2015).

1.3.2 Parabolic Troughs

In parabolic trough power plants, a series of curved mirrors are placed in a field of long rows which focuses the solar radiation onto a pipe in the focal point of the curve. The pipe carries either steam or storage medium (Tweidell et al., 2006). Similar to central receiver system, if the TES system is used then heat is transferred to water through heat exchangers. If not, water will run through the pipes at the focal point of the parabolic troughs. In either case, the steam is used in a standard Rankine cycle. The next figure shows an example of a CSP plant using parabolic troughs with a TES system.

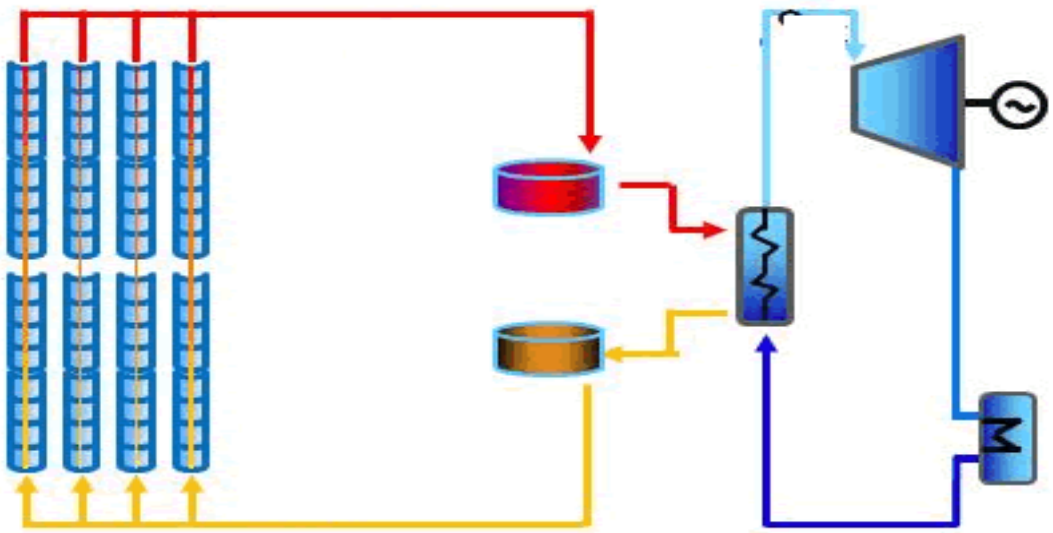

Figure 3: Parabolic troughs CSP plant (Cekirge et al., 2015).

1.3.3 Advantages and Disadvantages

Both central tower and trough systems have their own advantages and disadvantages. The central receiver CSP plant is, however, generally found to be the superior design. First, the central receiver system can be built over a rough terrain with minimal grading because each heliostat can focus the sunbeams using its dual axis configuration (Cekirge et al., 2015). This means there is higher flexibility where each heliostat is independent from the surrounding heliostats. Second, central receivers can be run at higher temperatures and pressures, which result in higher thermodynamic efficiency (Cekirge et al., 2015). Moreover, the flat heliostats used in central receivers are cheaper to manufacture which reduces the overall cost (Cekirge et al., 2015). Finally, the parasitic losses in the parabolic trough CSP plants are higher because of the very long length of piping used for fluid transfer. This results in both heat losses and pressure drop (Cekirge et al., 2015). The principal disadvantage of towers is the relative lack of commercial experience compared to parabolic troughs, although a number of recent field demonstration plants is addressing this issue. Therefore, the focus of this study will be on central receiver CSP plants.

1.4 Thermal Energy Storage (TES)

As discussed earlier in this chapter, one of the most difficult problems facing solar energy is the intermittency of energy production. One possible solution that has

already been applied to CSP plants is thermal energy storage. Thermal energy storage for CSP plants works by saving some of the excess energy during the day to be used at night. TES systems have the potential to reduce the mismatch between electricity supply and demand by supplying electricity over longer periods. In general, there are some technical requirements and criteria that define a good TES system. According to Abedin some of these requirements are (Abedin, 2010):

- Storage medium must have a high storage capacity by having a high potential energy density.
- The medium must be mechanically and chemically stable.
- The medium must be able to go through multiple charging and discharging cycles without significant degradation.
- The heat transfer between the storage medium and the working fluid (steam in CSP plants) must be high and there must be a high degree of compatibility between storage medium, heat exchangers, and the fluid.
- The system should have low thermal losses and should be easy to control.

1.4.1 Classification of TES systems:

There are three different types of thermal storage systems: sensible, latent, and thermochemical (Abedin, 2010). Sensible TES systems work by heating a storage medium and then later releasing the energy through heat transfer interactions (Abedin, 2010). For example, in CSP plants, two-tank molten salt systems are commonly used as a TES system (Tyner et al., 2014). Cold salt is pumped to the tower where it is heated and then it is directed to the hot (insulated) tank where it is stored for few hours after sunset (Tyner et al., 2014). The hot salt is then later used to raise steam.

The various latent TES systems work by storing/releasing the energy using a phase-change for a single material (Abedin, 2010). The generally greater energy storage capacity for latent heat systems relative to sensible heat systems leads to smaller system sizes for latent heat systems for the same storage capacity (Abedin, 2010). However, latent TES medium needs to be stored at the charging temperature, and phase change materials used in latent TES systems, for example paraffin, can be

corrosive (Abedin, 2010). Also, phase change materials used in such systems suffer from performance degradation after a moderate number of cycles (Tyner et al., 2014).

Thermochemical TES systems work by storing energy in an endothermic disassociation reaction, and the heat is recovered during the reverse exothermic chemical reaction (Abedin, 2010). A typical thermochemical storage medium has higher energy storage density compared to other types of TES systems. Another advantage is that thermochemical TES system can be used to store energy for longer periods with minimal heat loss (Abedin, 2010). Table 1 provides a comparison between the various TES systems.

Table 1: Comparison between TES systems (Pardo et al., 2014).

	Sensible heat storage system	Latent heat storage system	Thermochemical storage system
Energy density	Small	Medium	High
Volumetric density	~50 kWh m^{-3} of material	~100 kWh m^{-3} of material	~500 kWh m^{-3} of reactant
Storage temperature	Charging step temperature	Charging step temperature	Ambient temperature
Storage period	Limited (thermal losses)	Limited (thermal losses)	Theoretically unlimited
Transport	Small distance	Small distance	Theoretically unlimited
Maturity	Industrial scale	Pilot scale	Laboratory scale
Technology	Simple	Medium	Complex

As can be seen from the table above, thermochemical TES systems have several advantages, especially in the energy density, which is 5 to 10 times higher than that of the sensible and latent TES systems, respectively. Also, thermochemical systems store their energy at ambient temperature, which minimizes sensible heat loss. Also, the storage period for thermochemical system materials are theoretically unlimited and the materials can be transported to other locations. However, there are some drawbacks for thermochemical TES system such as the fact that it is still in the early ages of research, and the system is more complex to build than sensible and latent TES systems. Because thermochemical TES system has only been tested in laboratories, the objective of this paper is to explore the thermochemical TES option

on a utility-scale solar tower CSP plant by conceptually designing a reactor and integrating it with a standard Rankine cycle.

Chapter 2: Thermochemical Thermal Energy Storage System

A generalized thermochemical reaction that would be used in energy storage can be expressed as shown in Figure 4 by C+ heat ↔ A +B. Commonly a solid-gas reaction happens where C is solid, A is usually a solid and B is usually a gas. There are three steps for the thermochemical reaction: namely (1) charging, (2) storage, and (3) discharging (Abedin, 2010).

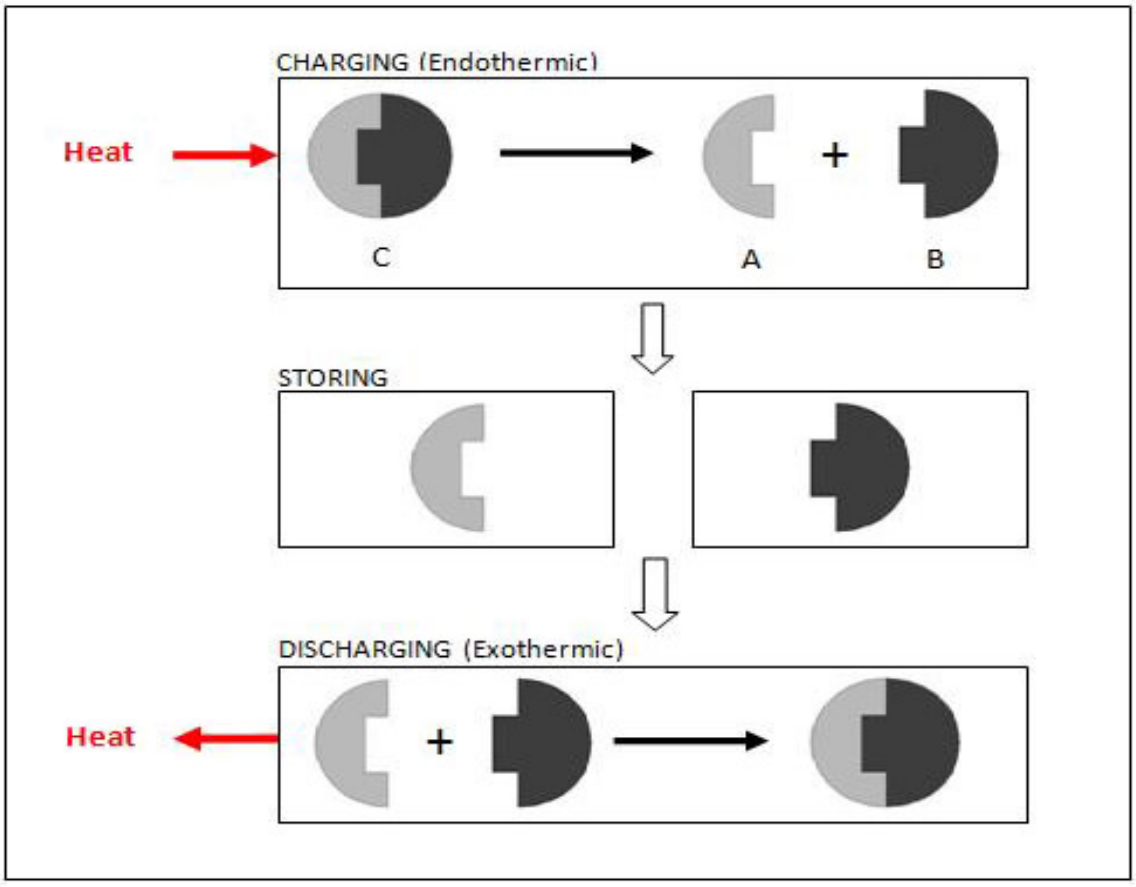

Figure 4: Reversible thermochemical reaction showing the charging, storing and discharging steps.

2.1 Thermochemical reaction steps

2.1.1 Charging

In this step, an endothermic reaction takes place where heat is supplied to C via renewable sources or fossil fuels in order to disassociate C into A and B. This heat is equivalent to the enthalpy of reaction plus the sensible heat needed to bring the reactants to the disassociation temperature (Felderhoff et al., 2013).

2.1.2 Storing

Following the disassociation step, the products A and B are separated and stored. Usually the products are stored at ambient temperature which ensures minimal heat loss caused by the cooling down of the products. In addition, stored energy can be lost by degradation of the stored products (Felderhoff et al., 2013).

2.1.3 Discharging

The discharging step is an exothermic reaction where reactants A and B are combined at specific conditions of temperature and pressure. If these conditions are met, product C will be recovered as well as the original heat supplied at the charging process.

2.2 Requirements for thermochemical TES systems

As shown in the last chapter, thermochemical TES systems have a good potential for storing thermal energy for longer periods than direct thermal storage systems (either based on sensible or latent heat storage). To design a thermochemical TES system, there are four necessary technical disciplines that should be characterized:

2.2.1 Chemistry

Understanding the chemistry behind the selected reaction is at utter most importance. The reaction is understood by studying the reversibility of the reaction, reaction rate and kinetics, the needed operation conditions and whether a catalyst is needed (Pardo et al., 2014).

2.2.2 Materials

Characterizing the materials involved in the reaction (i.e., reactants, products, and byproducts) is very important. For example, the reaction might involve a high enthalpy change and a high energy density, but the products of the reaction are corrosive. This will make it extremely difficult to build the system containing that reaction. Agents that are compatible with inexpensive materials of construction are desirable.

2.2.3 Heat transfer

The main purpose of TES systems is to store energy when it is available and release it when it is needed. Therefore, the heat transfer characteristics associated with both the charging and discharging process must be understood to correctly design

the reactor. This requires matching the intensity of the concentrated solar heat source with the rate at which heat can be absorbed by the reacting system. Thermodynamic considerations are needed to ensure that the reaction takes place at an optimum temperature.

2.2.4 Process and System analysis

Finally, an analysis of the technical and economic feasibility, the cost and benefit and the safety of the process must be performed. In general, after gathering all the information from these four technical areas, the design of the thermochemical TES system can be specified.

2.3 Possible Candidates

Thermochemical TES systems that work in medium to high temperatures (300-1100 °C) can use materials from the following families:

2.3.1 Hydrogen System: Metallic Hydrides

When a disassociation reaction happens in this family of materials, a metal is separated from hydrogen in an endothermic reaction. Energy is released when the reverse reaction happens in an exothermic manner. One material from this family that could be used for TES applications in CSP plants is MgH_2 via the following reaction (Bogdanovic et al., 1987):

$$MgH_{2(s)} + \Delta H_r \leftrightarrow Mg_{(s)} + H_{2(g)} \quad \text{with } \Delta H_r = 75\text{kJ mol}^{-1}$$

The working temperature for this reaction is between 523 K and 773 K while the partial pressure for hydrogen is in the range of 1 to 100 bar (Bogdanovic et al., 1987). Some of the advantages and disadvantages of this system are shown in Table 2. From the table, it can be seen that the system has high reversibility. However, the high operating pressure, slow reaction kinetics and the need for doping represent disadvantages.

Table 2: MgH_2 system advantages and disadvantages (Pardo et al., 2014).

	Advantages	Disadvantages
MgH_2 system	- Reversibility of the reaction (600 cycles) - No by-products - Gas-solid product separation - Experimental feedback	- Slow reaction kinetics - Operating pressure (up to 100 bar) - Need for Fe- or Ni-doping - Sintering - H_2 storage

2.3.2 Redox System

One of the materials from this family is cobalt oxide as shown in the following reaction (Pardo et al., 2014):

$$2Co_3O_{4(s)} + \Delta H_r \leftrightarrow 6CoO_{(s)} + O_{2(g)} \quad \text{with } \Delta H_r = 205 \text{ kJ mol}^{-1}$$

The working temperature of this reaction is between 973 to 1123 K with partial pressure for oxygen between 0 to 1 bar (Pardo et al., 2014). This reaction has high reversibility, high reaction enthalpy and easy to separate solid-gas reaction. However, the experimental understanding of this system is minimal, and the products are toxic and expensive (Pardo et al., 2014). A list of advantages and disadvantages are shown in the Table 3.

Table 3: Co_3O_4 system advantages and disadvantages (Pardo et al., 2014).

	Advantages	Disadvantages
Co_3O_4 system	- No catalyst - O_2 as a reactant - High reaction enthalpy - No by-product - Gas-solid reaction (easy separation) - Reversibility of the reaction (~500 cycles)	- Little experimental feedback - O_2 storage - Toxicity of products - Cost of products

2.3.3 Carbonate System

The reaction temperature of this family of materials is higher than 723 K (Pardo et al., 2014). One example is the disassociation of $CaCO_3$. After the endothermic reaction, CO_2 will form and it must be stored securely without leakage. One example from this family is $CaCO_3$ that react as (Barker, 1973):

$$CaCO_{3(s)} + \Delta H_r \leftrightarrow CaO_{(s)} + CO_{2(g)} \quad \text{with } \Delta H_r = 178 kJ\ mol^{-1}$$

The working temperature for this reaction ranges between 973 to 1273 K, and the CO_2 partial pressure goes up to 10 bars (Barker, 1973). It can be seen that the temperatures are higher than the typical range for CSP plants. The advantages and disadvantages of this reaction are listed in the Table 4 below (Pardo et al., 2014). As can be seen from the table, this reaction has a high energy density and it is a solid-gas reaction, which makes separation of the products relatively easy. On the other hand, the rate of the reaction slows when agglomeration and sintering affect the solids and Ti-doping is needed to make it more efficient.

Table 4: $CaCO_3$ system advantages and disadvantages (Pardo et al., 2014).

	Advantages	Disadvantages
$CaCO_3$ system	- No catalyst - Industrial experience with limestone production. - High energy density - No by-product - Gas-solid reaction (easy separation) - Availability and low cost	- Agglomeration and sintering - Poor reactivity - Change of volume (105%) - Need for Ti- doping - CO_2 storage

2.3.4 Hydroxide System

Materials from this family are considered the best candidates for TES systems in CSP plants because the working temperature ranges from 523 to 723 K and the system operates under low pressure (Pardo et al., 2014). There are two good candidates

from this family: $Mg(OH)_2$ and $Ca(OH)_2$. $Mg(OH)_2$ works at intermediate temperatures (370 to 440 K) which will not be good for CSP applications (Pardo et al., 2014). The other material is $Ca(OH)_2$, which works at 723 to 833 K and H_2O partial pressure of 0 to 2 bar (Criado et al., 2014). The reaction is shown below:

$$Ca(OH)_{2(s)} + \Delta H_r \leftrightarrow CaO_{(s)} + H_2O \quad \text{with } \Delta H_r = 109 \text{ kJ mol}^{-1}$$

This system has high energy density, high number of reversible cycles, nontoxic products and 10 years of experimental application. Also, the reagents are very inexpensive. However, agglomeration and sintering are noticed during the reversible reaction (Pardo et al., 2014). Advantages and disadvantages are listed in the following table.

Table 5: $Ca(OH)_2$ system advantages and disadvantages (Pardo et al., 2014).

	Advantages	Disadvantages
$Ca(OH)_2$ system	- No catalyst - Nontoxic products - High energy density - No by-product - Gas-solid reaction (easy separation) - Availability and low cost - 10 years of experimental feedback - Reversibility of the reaction (~1000 cycles) - Low operating pressure	- Agglomeration and sintering - Change of volume (95%) - Low conductivity

2.3.5 Ammonia System

Two ammonia systems have been studied for TES applications. The first is the decomposition of NH_4HSO_4 and the second is the decomposition/synthesis of NH_3. The first works at 690 K temperature and 1.46 atm, it does not need a catalyst, and has high energy density as shown in the reaction (Wentworth et al., 1976):

$$NH_4HSO_{4(l)} + \Delta H_r \leftrightarrow NH_{3(g)} + H_2O_{(g)} + SO_{3(g)} \quad \text{with } \Delta H_r = 336 \text{ kJ mol}^{-1}$$

Some of the advantages and disadvantages are shown in Table 6.

The second reaction is the direct decomposition of NH_3.

$$2NH_{3(g)} + \Delta H_r \leftrightarrow N_{2(g)} + 3H_{2(g)} \quad \text{with } \Delta H_r = 66.9 \text{ kJ mol}^{-1}$$

This reaction operates in the temperature range of 673 and 973 K and requires high operating pressure (80 to 200 bar) (Tempkin et al., 1940). One advantage of this reaction is the large experimental database that exceeds 40 years (Pardo et al., 2014), as can be seen in Table 7. The enthalpy of reaction is low to moderate.

Table 6: NH_4HSO_4 system advantages and disadvantages (Pardo et al., 2014).

	Advantages	Disadvantages
NH_4HSO_4 system	- No catalyst - High energy density - Gas-solid reaction (easy separation)	- Little experimental feedback - Corrosive products - Toxicity of products

Table 7: NH_3 system advantages and disadvantages (Pardo, et al., 2014).

	Advantages	Disadvantages
NH_3 system	- 100 years of feedback for ammonia synthesis - Liquid at ambient temperature - No side reaction	- H_2 and N_2 storages. - Use of catalyst (Fe/Co). - High operating pressure. - Incomplete conversion of both forward and reverse reaction.

In summary, there are advantages and disadvantages for each system and the following figure summarize the temperature vs. the enthalpy of reaction for each system. CSP plants typically operate in temperature range 600 to 873 K, while

parabolic troughs can go up to 823 K and higher for central receivers (around 873 K) (Cekirge et al,. 2015). The ammonia systems have the highest mass energy density of the systems described, however they are not the best candidates because the NH_3 system has high operating pressure and low (or incomplete) reversibility. Similarly, the NH_4HSO_4 system is not attractive because it produces corrosive, toxic products and has had little industrial development. The MgH_2 system also has disadvantages in that the reactants need to be doped with Ni or Fe, it has slow reaction kinetics, and it requires a high operating pressure. For the $Ca(OH)_2$ system, the main drawback is particle agglomeration and sintering that reduce reactivity and thus limit the number of cycles the reaction can go through. However, this problem has been addressed as is described in the next section where the reagents can now be used for at least 1000 cycles. Beyond this, the $Ca(OH)_2$ system has many advantages such as moderate mass energy density, good reversibility, good industrial experience, no by-products, no corrosive or toxic products and it is based on very low cost materials. From Figure 5, compared to other systems in the range of 600 to 900 K, $Ca(OH)_2$ system has the lowest energy density, and the other systems might seem like better candidates. However, the other systems have disadvantageous operational conditions such as high pressure or corrosive products that makes $Ca(OH)_2$ a better choice. From the graph and from the figures in Tables 2 to 7, the $Ca(OH)_2$ system can be projected to be a very favorable candidate for use as thermochemical TES medium for CSP plants applications.

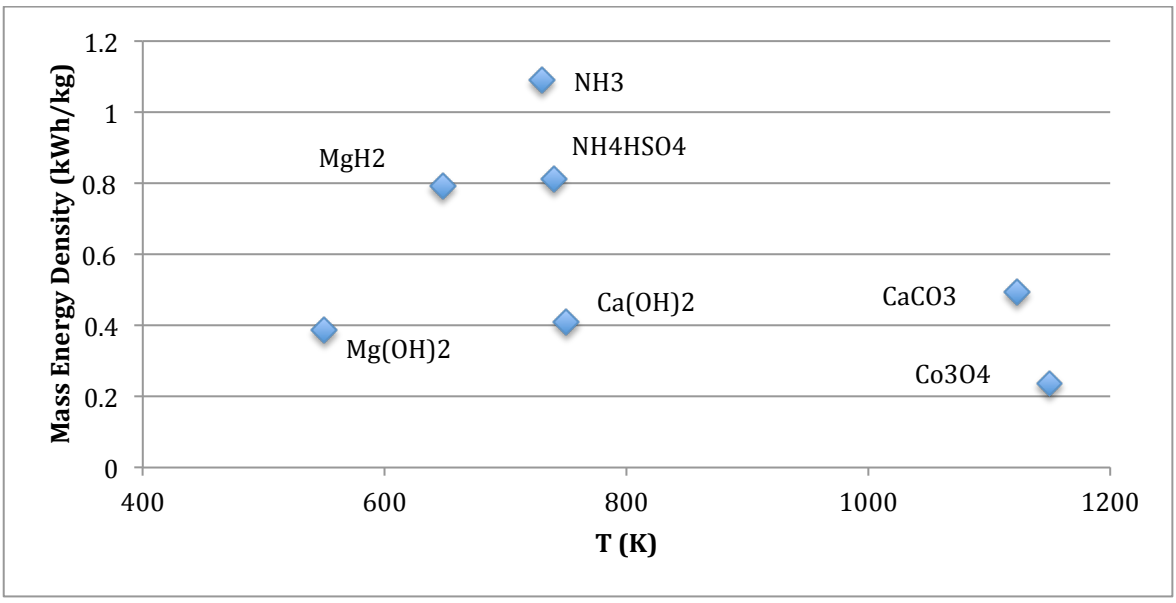

Figure 5: mass energy density vs. temperature

2.4 Calcium Hydroxide System

As discussed in the last section, $Ca(OH)_2$ system has many advantages and some drawbacks. One of the main concerns with this system is the agglomeration and sintering of the particles, which can reduce the reactivity after a large number of cycles. In Pardo's paper (2014), this reversible reaction could only perform 20 to 40 cycles. For CSP plants where the reaction goes through one cycle a day, the TES medium would require changing every thirty days on average. This is not practical from technical and economic standpoints. From the technical standpoint this means more time will be lost in the process of removing the old material from this system and replacing it with the fresh reagent. As a result, less energy will be produced and the overall plant performance will be reduced. From the economics standpoint, a monthly recurring payment for replacing the materials has to be made. Second, changing reagent will result in plant downtime. Lastly, there will be costs associated with the fresh reagent, and the labor needed to perform the replacement.

However, Criado (2014) has stated that CaO can be fully hydrated into $Ca(OH)_2$ within 15 seconds at 100 kPa absolute, 455 °C and a particle diameter in the range of 100 to 200 μm. This is a faster hydration rate than most of the results presented in the literature. This faster rate is the result of special care taken during the experimental setup to eliminate diffusional resistances (Criado et al., 2014).

Likewise, the dehydration process also took around 15 seconds at 100 kPa absolute and 560 °C with the same particle diameter (Criado et al., 2014). Furthermore, hydration/dehydration tests with 100 -200 μm particles diameter up to 32 cycles showed no loss in degree of conversion, which confirms the results reported by Rosemary with 1171 hydration/dehydration cycles (Rosemary et al., 1979). Therefore, assuming the same conditions in this experiment are followed, the important concern regarding reagent lifetime for the $Ca(OH)_2$ system is largely reduced, and this system would be ideal to use for TES applications in CSP plants.

Chapter 3: Reactor Design

As mentioned in Chapter 2, thermochemical TES systems have only been tested at laboratory scale. Thus this chapter focuses on the design of a utility-scale application for the calcium hydroxide system. The reactor must be able to hold both charging and discharging reactions. For the charging reaction, the reactor must be able to absorb solar energy and supply it to $Ca(OH)_2$ in order to promote conversion into CaO and H_2O, while for the discharging reaction, the reactor must be able to extract the heat generated when CaO reacts with H_2O. In both reactions, the reactor must provide good gas-solid mixing during the reaction, and good gas-solid separation after the reaction.

3.1 Type of Reactor

Selection of the appropriate reactor type is very important for the process. Economics dictate that the size be as small as possible. This requires (1) that high heat transfer rates be employed, and (2) that high mass transfer rates between the reagents be available. The common reactor system that provides the highest heat and mass transfer rates is the fluidized bed. The two most common formats are the bubbling fluidized bed and the circulating fluidized bed. We will explore both options.

3.1.1 Fluidized Bed Reactors

Fluidized bed reactors can be classified based on the flow velocity. Low flow velocities result in a bed of stationary particles where the gas flows through the voidage. These are termed static packed beds. If the flow velocity is increased to a point where the fluid drag is equal to the weight of particles, the solids start behaving like liquid and this velocity is called the minimum fluidization velocity, U_{mf} (Grace et al., 1997). For Group B and D particles (from 40 μm to above 600 μm (Basu, 2015)) any increase in the gas flow beyond the minimum fluidization velocity will cause the extra gas to flow in the form of bubbles (Grace et al., 1997).

Fluidization is defined as the operation through which solids are transformed into a fluid-like state through contact with either a gas or a liquid. If the gas flow is increased further, solids will start entraining into the reactor flow, and the system becomes a circulating fluidized bed (CFB) (Basu, 2015). If the flow velocity is

increased further, the solids will be entrained faster leading to dilute-phase reactors (Basu, 2015). Table 8 below gives a detailed comparison between low-velocity beds, circulating beds and dilute-phase reactors.

Table 8: Comparison between fluidized bed systems (Grace et al., 1997).

	Low-velocity fluidized bed reactor	Circulating fluidized bed reactors	Dilute-phase transport reactors
Particle Histories	Particle spend substantial time in the main reactor vessel (minutes or hours) Occasional excursion through cyclone or standpipe	Particles pass repeatedly through the recirculating system; residence time in the main vessel for each circuit is counted in seconds	Once-through system
Hydrodynamic regime	Bubbling, slugging or turbulent fluidization, with distinct upper interface	Usually fast fluidization, through bottom of the reactor may correspond to turbulent fluidization conditions or even bubbling	Dilute transport conditions
Superficial gas velocity	Generally below 2 m/s	Usually 3 to 16 m/s	Usually 15 to 20 m/s
Mean particle diameter	0.03 to 3 mm	0.05 to 5 mm	0.02 to 0.08 mm
Net circulation flux of solids	Low, generally 0.1 to 5 kg/m^2s	Substantial, e.g. 15 to 1000 kg/m^2s	Up to ~ 20 kg/m^2s
Voidage	0.6 to 0.8 in bed	0.8 to 0.98	Generally > 0.99
Gas mixing	Substantial axial dispersion; complex two phase behavior	Some gas downflow near walls typically results in intermediate gas mixing	Very little axial dispersion

As can be seen from Table 8, CFB reactors are favorable for many reasons. First, the degree of mixing between solids and gas in CFBs is higher than the other types of fluidized reactors. Second, because of the better mixing, fewer feed points are needed and the temperature inside the reactor is more uniform (Grace et al., 1997). While CFB reactors tend to have a higher capital cost, they satisfy the technical requirement in giving the best mixing between solids and gas (Grace et al., 1997). Advantages and disadvantages of CFB reactors are listed in the Table 9.

Table 9: Advantages and disadvantages of CFB (Grace et al., 1997)

Advantages	Disadvantages
Improved gas-solid contacting given the lack of bubbles	Increased overall reactor heights
Reduced axial dispersion of gas	Higher capital cost
Reduced cross-sectional area given the higher superficial velocities	Added complexity in designing and operating recirculating loop
No region like the freeboard region of low-velocity beds where there can be substantial temperature gradients	Increased particle attrition
Less tendency to show particle segregation and agglomerations	
Because of superior radial mixing: • Fewer solid feed-points are needed • Uniform temperature	
Higher solids flux through the reaction	

3.2 Circulating fluidized bed (CFB)

Circulating fluidized beds consist of: a riser (furnace) where the solid material is moving toward a gas-solid separator (cyclone). From the cyclone, the solids go through a returning leg (loop seal) back toward the riser (Basu, 2015).

In general, the fluidizing medium (steam) enters from the bottom of the riser and the solid feed ($Ca(OH)_2$/ CaO) is added from feed-points higher in the system. In the core of the reactor particles tend to go upward while near the walls particles agglomerate forming clusters going downward (Basu, 2015). The clusters fragment while going downward gets picked up by the upward flow. This motion increases the mixing leading to an even temperature distribution and a better reaction (Basu, 2015). The particles exit the riser as an entrained flow and move to a gas-solid separator. Steam leaves the reactor while the solid returns to the riser through the loop seal in order to go through another loop.

3.2.1 CFB Design

The design of a circulating fluidized bed (CFB) reactor requires several steps. The first focuses on the nature of the gas-solid system, including the thermodynamics of the reaction, and reaction kinetics (Basu, 2015). This information allows the gas velocity and the flow rates to be calculated and the required residence time and the riser height to be determined. Finally, the cyclone and downcomer are designed. The next several sections cover the design process step by step.

3.2.2 Data Gathering

The reactor must supply heat to the endothermic reaction through the absorption of heat from reflected sunbeams, and release the heat to raise steam at a later time via the exothermic reverse reaction. As will be explained in Section 4.1, these two requirements cannot be accomplished in one reactor. Thus, two reactors will be used, one for each reaction.

During the day, the endothermic reaction (charging process) occurs where $Ca(OH)_2$ is heated and CaO and steam are produced as:

$$Ca(OH)_{2(s)} + \Delta H_r \leftrightarrow CaO_{(s)} + H_2O_{(g)} \quad \text{with } \Delta H_r = 109 \text{ kJ mol}^{-1}$$

As discussed earlier, the kinetics for this reaction specifies a reaction temperature of 560 C and pressure of 100 kPa absolute and it takes around 15 seconds for the reaction to occur. The heating medium used to heat calcium hydroxide is steam as shown in the following reaction, in addition to the heat supplied to the reaction through the reactor walls.

$$Ca(OH)_{2(s)} + H_2O_{(g)} \leftrightarrow CaO_{(s)} + 2H_2O_{(g)}$$

On the other hand, the exothermic reaction takes place during the night at 450 C and 100 kPa absolute. The reactor must be insulated in order to trap the heat generated from the reaction inside and supply it to water/steam running contained in the water-walls inside the reactor. There are some parameters that need to be specified to design the reactors for both the endothermic and exothermic reactions, such as the gas velocity, gas-solid flow rates, and the reactor diameter.

To identify the flow rates for both solids and gas, the turbine is specified to produce 100 MW_e. For gas, there are two different flow rates, the first is the one running the turbine and the second is the amount needed for the thermochemical reaction. The calculations for the gas flow rates running the turbine are shown in Chapter 4. For the solid flow rates, since heat generated from the CaO reaction with steam is the source of heating for steam inside water-walls that will be running the turbine, then from total amount of heat needed, the flow rate of CaO is calculated. Since the relationship between $Ca(OH)_2$ and CaO in the thermochemical reaction is one to one, then the flow rate of $Ca(OH)_2$ in kmole/s is the same as the flow rate of CaO. As will be shown in Chapter 4, the total amount of heat that needs to be released in the exothermic reaction can be provided by 4.3 kmole/s of CaO, thus, the flow rate for $Ca(OH)_2$ is 4.3 kmloes/s as well. Knowing the molecular weight for each element in the reaction, the mass flow rates can be converted to kg/s, as shown in the Table 10.

Table 10: Mass flow rates for the endothermic reaction

	Flow rate (kmol/s)	Molecular weigh (kg/kmol)	Flow rate (kg/s)
$Ca(OH)_2$	1	74.093	74.093
H_2O	1	18	18
CaO	1	56.08	56.08

After knowing the flow rates for calcium hydroxide and steam, the gas velocity is calculated.

3.2.3 Gas Velocity

The gas velocity has to be higher than the minimum velocity at which fast fluidization happens; this minimum velocity is called transport velocity (Basu, 2015). The fluidization velocity is higher than the terminal velocity for a single particle and will empty a column (riser) from solids during a certain amount of time. If the velocity is decreased, the time taken to empty the column will increase gradually until the velocity reaches a critical point where there will be a sudden increase in time. This velocity is called transport velocity, U_{tr}, and it is empirically calculated as (Basu, 2015):

$$U_{tr} = 1.45 \frac{\mu}{\rho_g d_p} Ar^{0.484}, \quad 20 < \text{Ar} < 50{,}000$$

Where, Ar= Archimedes number = $\frac{\rho_g(\rho_p - \rho_g) g d_p^3}{\mu^2}$

μ= dynamic viscosity

ρ= density (p for particles; g for gas)

d_p= Particle's mean diameter.

To find the transport velocity, properties of gas and solid particles must first be specified. These are shown in Table 11. As discussed in Chapter 2, the mean diameter of the particles is taken to be 200 μm. The properties of the steam are taken at 100 kPa absolute and two different temperatures: 455 C for the exothermic reaction and 560 C for the endothermic reaction.

Table 11: Solids and gas properties

	$Ca(OH)_2$	CaO	H_2O
Density (kg/m^3)	2210	3350	0.2602 @ 560 C 0.2999 @ 455 C
Dynamic viscosity (kg/m-s)	--	--	3.1E-5
Particle diameter (μm)	100 – 200	100 – 200	--

For CaO particles, Ar= $\frac{(200*10^{-6}m)^3(3350-0.2999)kg/m^3(0.2999)kg/m^3(9.81)m/s^2}{(2.734*10^{-5}Pa-s)^2} = 105.47$

from that the transport velocity can be calculated as flow:

$$U_{tr} = 1.45\ \frac{(2.734 * 10^{-5} Pa - s)}{(0.2999) kg/m^3 (200 * 10^{-6}) m}\ (105.47)^{0.484} = 6.3\ m/s$$

The superficial velocity, U, is known to be higher than U_{se}, which is known as the significant solids entrainment velocity (Grace et al., 1997) as:

$$U > U_{se} > U_{tr}$$

Where $U_{se} = 1.53\ \frac{\mu}{d_p \rho_g}\ Ar^{0.5} = 1.53\ \frac{(2.734 * 10^{-5} Pa - s)}{(0.2999) kg/m^3 (200 * 10^{-6}) m}\ (105.47)^{0.5} = 7.16\ m/s$

Therefore, the superficial velocity is set to be equal to 7.5 m/s. Since the residence time for the exothermic reaction is 15 seconds, the height of the reactor is equal to the superficial velocity multiplied by residence time. This will give a height equal to 112.5 meters. This is height is not acceptable and needs to be shortened for many reasons. For example, the reactor with this height will cast a shadow on the heliostats and this will decrease the efficiency. Also, it is not economically feasible to build a 112.5 meters long reactor. The proposed solution is to have the solids circulate between the riser and downcomer three times before leaving the reactor, which means each circulation will take 5 seconds and the total height of the reactor will be 37.5 meters.

3.2.4 Reactor Diameter

To specify the required diameter of the reactor, the total amount of solids inside the reactor must be known and from that the amount of gas needed can be calculated. In the first loop, a certain amount of $Ca(OH)_2$ enters the reactor per second and this will leave the riser and enter the cyclone, and then be sent back to the riser. This amount is 4.3 kmole of $Ca(OH)_2$ as will be explained in the next chapter. When it returns to the riser it will be joined by another 4.3 kmoles of $Ca(OH)_2$ entering the reactor. Both amounts will continue the loop until they return to the riser again, where they will be joined by a third 4.3 kmole of $Ca(OH)_2$. After leaving the cyclone, the 4.3 kmoles of $Ca(OH)_2$ that have been in the system since the first loop, would be fully dehydrated to CaO by this time. All solids after leaving the cyclone will enter a density-based solid separator device, where CaO particles and $Ca(OH)_2$ particles will be separated and CaO particles will be picked out of the system. The rest of the $Ca(OH)_2$ will return to the riser and will be joined by a new 4.3 kmoles of $Ca(OH)_2$.

So after the third loop the process keeps repeating itself. To summarize, at each second, 4.3 kmoles of $Ca(OH)_2$ enter the riser, 8.6 kmoles of $Ca(OH)_2$ return to the riser, and 4.3 kmoles of CaO leave through the density-based solid separator. The process is summarized below in Table 12 for the first 4 loops where it starts repeating itself after the third loop.

Table 12: First 4 loops of solids inside CFB.

	Entering	Returning	Leaving
1st loop	4.3 kmole	--	--
2nd loop	4.3 kmole	4.3 kmole	--
3rd loop	4.3 kmole	8.6 kmole	4.3 kmole
4th loop	4.3 kmole	8.6 kmole	4.3 kmole

Since the solids stay inside the reactor for five seconds, the total amount of $Ca(OH)_2$ inside the reactor at any given instant is

$$5\ sec * \frac{4.3\ kmole}{sec} * 3 = 64.5\ kmole\ Ca(OH)_2 = 4779\ kg\ Ca(OH)_2$$

On the other hand, at each second 4.3 kmoles of steam enters the reactor, 4.3 kmole will be generated from the reaction and 4.3 kmole leaves, leading to a total of 6*4.3= 25.8 kmoles being inside the reactor at all times, which is equal to 464.4 kg of steam. Knowing the amount of solids and gas inside of the reactor at all times, the diameter of the reactor can be found as shown in the following equation:

$$V = \frac{\pi D^2 H}{4} = \frac{m}{\rho}$$

where: V= volume of the reactor. D= diameter of the reactor,

H= height of the reactor m = total mass ρ = density.

The total volume of the reactor is equal to the volume of solids and the volume of steam combined. The volume of $Ca(OH)_2$ is

$$V_s = \frac{m_s}{\rho_s} = \frac{4779\ kg}{2210\ kg/m^3} = 2.16\ m^3$$

The volume of the steam is

$$V_g = \frac{m_g}{\rho_g} = \frac{464.4\ kg}{0.2602\ kg/m^3} = 1784.78\ m^3$$

Therefore the total volume is equal to 2.16 m^3 plus 1784.78 m^3 = 1786.94 m^3. From that, the diameter is

$$D = \sqrt{\frac{4V}{\pi H}} = \sqrt{\frac{4(1784.78\ m^3)}{\pi(37.5m)}} = 7.79\ m$$

The diameter will be set to be 8 m in order to include the volume occupied by water-walls (water-walls details will be discussed in next chapter).

There is a difference in diameter calculations for the exothermic reaction because of the difference in the amount of gas inside the reactor. In the endothermic reaction, 4.3 kmole of H_2O is generated by the reaction at each second. Therefore, the amount of H_2O for the exothermic reaction is:

$$5\ sec * \frac{4.3\ kmole}{sec} = 21.5\ kmole\ H_2O = 387\ kg\ H_2O$$

While the amount of CaO particles inside the reactor at each second is 4.3 kmoles=3617.16 kg of CaO. Leading to the diameter for the endothermic reaction to be 7.2 m.

3.2.5 Gas-solid separator:

When gas and solid leave the reactor, they enter a gas-solid separator (cyclone). The most commonly used cyclone type is a cyclone with vertical axis, tangential inlet suspension, and upward axial discharge of gas as shown in the next figure (Basu, 2015). In this type of cyclone, solids and gas enter tangentially into the cyclone barrel forming two concentric vortices. With the density difference between solids and gas and with centrifugal forces effect on solids, the solids will be in the outer vortex, while the inner vortex is for gas. After going through number of loops inside the cyclone, the solids travel downward where the particles are collected by a standpipe. The gas vortex travels upward toward the vortex finder to leave the cyclone. The gas-solid separation process is shown in Figure 6 where the path of the solids is shown by dashed lines and the path of the gas is shown by the solid lines. For solids to leave the cyclone through the standpipe, they must have a particle size larger than a critical particle size to avoid being entrained by the gas. Nevertheless,

it is hard to define a specific cutoff particle size above which all solids will be captured and below which all the solids will be entrained. However, there is a theoretical particle diameter for which larger particles have higher probability of being captured and smaller particles have less probability (Basu, 2015). This theoretical diameter is given by:

$$d_{th} = \sqrt{\frac{9\mu L}{\pi N_c V_i (\rho_p - \rho_g)}}$$

Where, μ = dynamic viscosity V_i= inlet velocity

L= width of inlet duct ρ = density (g for gas and p for particles)

N_c= number of turns made by gas stream inside the cyclone (often taken as 5)

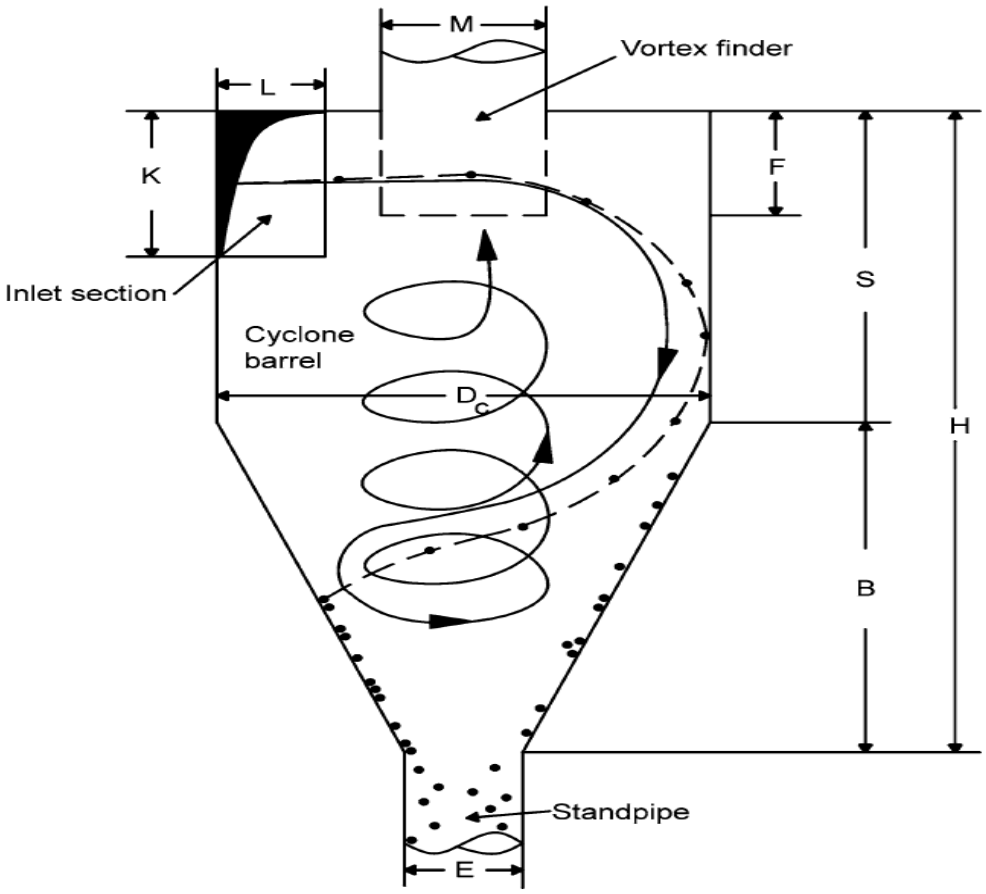

Figure 6: A cyclone showing the paths of solids and gas.

From the figure above, there are several dimensions that need to be specified in order to design the cyclone and most importantly is the diameter of the cyclone

denoted by D_c. Specifying the cyclone diameter leads to finding all the other dimensions shown in the figure because they all have been correlated to the cyclone diameter D_c as shown in Table 13. The last column of the table shows the ratios commonly used in common practice for CFB boilers. Since the data of this column are gathered from actual CFB boilers, it is preferable to work with these values. Since the ratios from the general CFB boiler column vary considerably, mean values are used for the calculations.

Table 13: Ratios of the dimensions of the cyclone related to the cyclone diameter, D_c (Basu, 2015).

	High throughput	General purpose	High efficiency	General CFB boiler
K/D_c	0.75	0.5	0.44	0.75-1.25
L/D_c	0.375	0.25	0.21	0.25-0.35
M/D_c	0.75	0.5	0.4	0.45-0.55
F/D_c	0.875	0.6	0.5	0.25-0.50
S/D_c	1.5	1.75	1.4	1.0-1.50
H/D_c	4.0	3.75	3.9	2.0-3.5
E/D_c	0.375	0.4	0.4	0.15-0.25

According to Basu (2015), the general approach to design a cyclone for CFB boiler purposes starts with choosing an inlet velocity, where typical values range from 20-30 m/s, and from that calculating the diameter and the other dimensions. After that, the cutoff particle size and the particle collection efficiency are calculated. The process is iterative. Starting with a 30 m/s entry velocity one checks to see if the cyclone diameter falls in the typical diameter range (the typical cyclone diameter range is from 0.5 to 8 m (Basu, 2015)). If not, a different trial value for velocity is used. The volumetric flow rate is then used to find the diameter:

$$Q = UA$$

Where, Q is the total volumetric flow rate

U is the entry velocity

A is the entry area

The total volumetric flow rate is equal to volumetric flow rate of steam plus the volumetric flow rate of the solids. The volumetric flow rate equals the total volume of gas (solid) divided by the time it takes inside the reactor (5 seconds):

$$Q_s = \frac{V_s}{t} = \frac{2.16\ m^3}{5\ s} = 0.432\ m^3/s$$

$$Q_g = \frac{V_g}{t} = \frac{1487.32\ m^3}{5\ s} = 297.46\ m^3/s$$

From Figure 6, the entry area is equal to length and width of the entry section (A= KL). From the general CFB boiler column in Table 12, $K/D_c = 1$, $L/D_c = 0.3$, therefor $A = 0.3\ D_c^2$.

$$D_c = \sqrt{\frac{Q}{0.3V}} = \sqrt{\frac{(297.46 + 0.432)\ m^3/s}{0.3(30\ m/s)}} = 5.75\ m$$

With the diameter of the cyclone being known now, the dimensions of the other cyclone parameters are calculated and are summarized in Table 14.

Table 14: Dimensions of the cyclone (Basu, 2015)

K	$1xD_c$	5.75
L	$0.3xD_c$	1.725
M	$0.5xD_c$	2.875
F	$0.375xD_c$	2.156
S	$1.25xD_c$	7.19
H	$2.75xD_c$	15.81
E	$0.2xD_c$	1.15

The particle collection efficiency is calculated by finding the d_{th} then dividing it by d_p and using Figure 7 to find the efficiency.

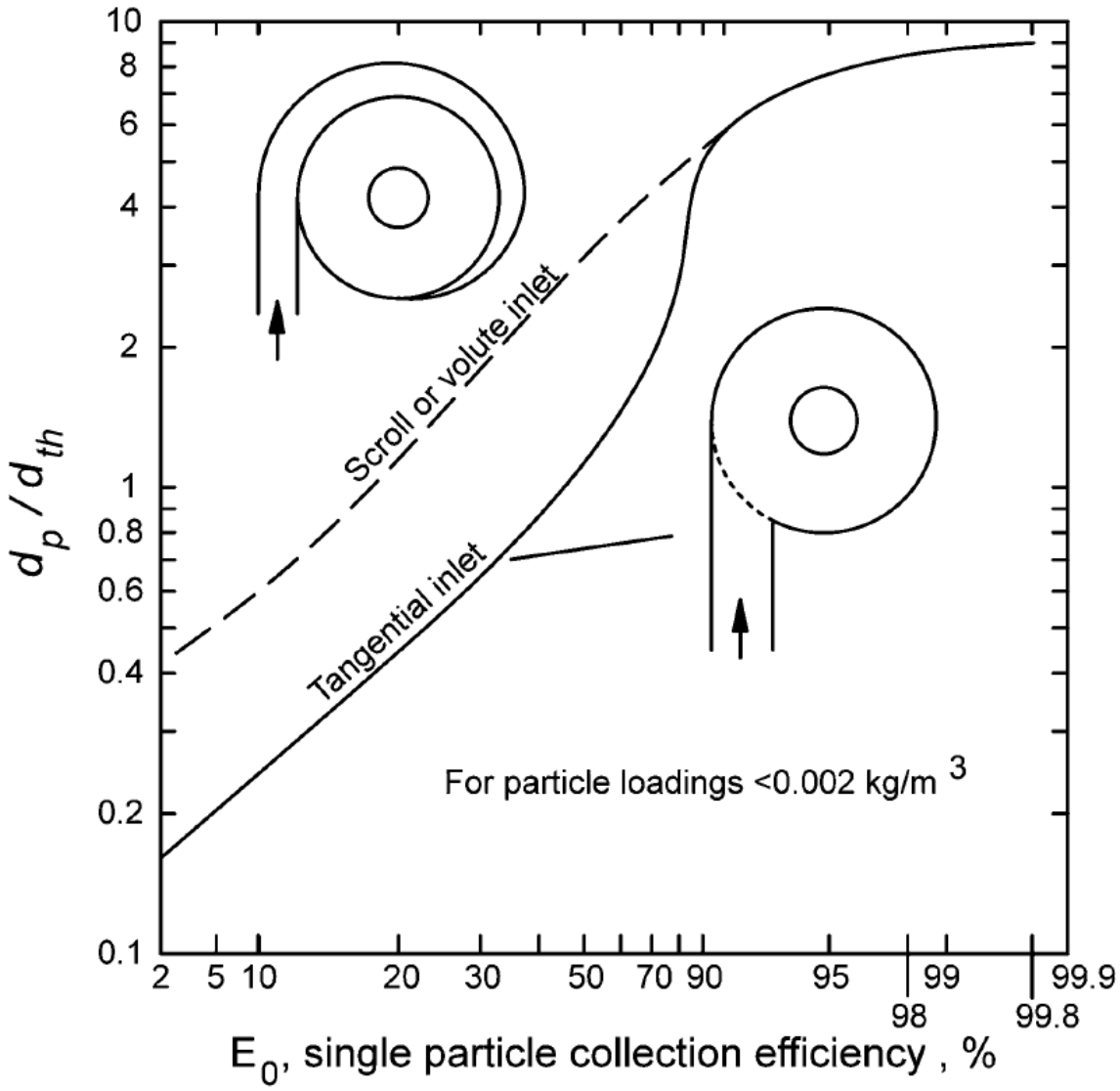

Figure 7: Particle collection efficiency vs. d_p/d_{th}

$$d_{th} = \sqrt{\frac{9\mu L}{\pi N_c V_i (\rho_p - \rho_g)}} = \sqrt{\frac{9(2.734 * 10^{-5} Pa - s) * (1.43\ m)}{5\pi(30\ m/s) * (3350 - 0.2602) kg/m^3}} = 15\ \mu m$$

$$\frac{d_p}{d_{th}} = \frac{200\ \mu m}{15\ \mu m} = 13.33$$

From Figure 7, the collection efficiency is higher the 99.9%. In other words, it can be safely assumed that the gas leaving the cyclone is free of solids.

3.2.6 Density-based Solid Separator

Since the solids coming out of the cyclone are mixed $Ca(OH)_2$ and CaO particles, a solid separator device must be used. Since the particles have the same diameter, it is necessary to use a solid separator device that can separate particles based on the difference in density. During the day, the density-based solid separator will pull CaO particles out the system and $Ca(OH)_2$ particles will be directed toward the loop seal in order to return to the riser for another loop. During the night, the opposite will happen where calcium hydroxide particles will be pulled out of the system while calcium oxide particles will go for more loops. Going from the endothermic to the exothermic portion of the process, the type of solids used ($Ca(OH)_2$/CaO) should not have any effect in changing the dimensions of the reactor because the effect of changing the amount of solid particles in the overall volume is negligible compared to the volume of gas.

3.2.7 Refractory Lining

Refractory linings are commonly used inside CFB boilers for its thermal and mechanical properties. Some of its special properties are (Basu, 2015):

- Providing thermal insulation, wear resistance, corrosion resistance, and easy control of heat absorption.
- Can easily be fabricated into complex shapes for cyclone applications.
- Very cost-effective barrier against erosion.

The refractory has to withstand the thermal and mechanical load inside the reactor, which is at 100 kPa absolute of compressive stress and 455 C. Also, it must be able to resist corrosion from steam and calcium oxide/hydroxide particles. Additionally, it must be able to maintain dimension stability after mechanical and thermal load cycles.

The modulus of rupture is used to measure the stress the refractory can take before breaking (Basu, 2015). For safety measures, it is assumed that the minimum modulus of rupture that can be used is 500 kPa absolute instead of 100 kPa. Table 15, compares different grades of refractory that could be used. According to the

Plibrco products specification sheets (2013), the presented grades satisfy the mechanical and thermal criteria.

Table 15: Different refractory grades and there thermal and mechanical properties

	Refractory Grade	Maximum Temperature (C)	Modulus of rupture (MPa)	Thermal conductivity (w/m-k)
1	PLICAST LWI-26	1400	1.47	0.442
2	PLICAST LWI-24	1350	1.47	0.419
3	PLICAST LWI-22	1200	0.98	0.302
4	PLICAST LWI-20	1100	0.88	0.256

To avoid losing some of the heat from the particles while they are in the downcomer, the whole reactor should be insulated including the riser and all parts of the downcomer. In order to know how much refractory is needed, two things must be known: the surface area it is covering, and the thickness of the refractory layer. For the riser, the surface area is found by knowing the diameter and the height of the riser, plus the surface area of the roof of the riser:

$$A_s = \pi DH + \frac{\pi D^2}{4} = \pi(7.2m)(37.5m) + \frac{\pi(7.2m)^2}{4} = 848.23 + 40.72 = 888.95\ m^2$$

The thickness of the refractory layer is found by using the equations for heat transfer in concentric cylinders as flows (Incropera, 2007):

$$r_2 = r_1 EXP[\frac{\Delta T\ k}{\ddot{q}\ r_1}]$$

where $\ddot{q}$ is heat flux.

k is thermal conductivity of the refractory layer

ΔT is the temperature difference between the inside surface of the refractory and its outside surface.

r_1 is radius of the reactor

r_2 is the radius of the reactor (r_1) plus the refractory layer thickness

The heat flux going through the refractory is set not to exceed 2% of the total heat inside the reactor, that is 7902 W/m^2 (the total amount of heat inside the reactor will be discussed in the next chapter). The outer surface of the refractory is set not to exceed 100 C, and the inner surface is set to be at the same temperature as the bed, that is 455 C. This leads to ΔT being equal to 355 C. For simplicity, all the other parts of the CFB will be assumed to have the same thickness as that required for the riser. For the cyclone, the surface area is equal to 262.24 m^2, which includes the walls and the roof of the cyclone excluding the vortex finder area. The standpipe and return leg are given a length of 2 m for each, which gives an area of 14.44 m^2 for both parts. Therefore, the total area for the downcomer is 276.68 m^2 and the total surface area for the whole reactor being 1165.63 m^2. Table 16 shows the thickness for each refractory grade discussed in the table above. Knowing the surface area and the thickness of the refractory layer, the volume is calculated and, consequently, the total mass and the final cost.

Table 16: refractory layer thickness and total cost

Refractory	Density (kg/m^3)	Thickness (m)	Volume of thickness (m^3)	Total mass (kg)	$/kg	Total Cost
PLICAST LWI-26	1300	0.0196	22.88	29746.70	1.675	$49,900
PLICAST LWI-24	1370	0.0186	21.69	29712.98	1.220	$36,300
PLICAST LWI-22	1170	0.0134	15.62	18276.44	1.543	$28,200
PLICAST LWI-20	950	0.0114	13.24	12575.91	2.015	$25,400

As can be seen from the table, the chosen grade is PLICAST LWI-20 because it has the lowest amount of material and the lowest cost between all the grades.

Specifying the refractory lining concludes the design process for the CFB reactor, and the next step is integrating this design into a power cycle. The next chapter will discuss the integration process in detail.

Chapter 4: Cycle Integration:

After designing the reactor and choosing the appropriate material for the charging and discharging processes, it is necessary to integrate it with a power generation cycle as in CSP plants in order to use the useful heat generated. The components of a CSP plants are as follows (Gil et al., 2010):

- Concentrator
- Receiver
- Power block unit
- Transport/ storage Media (optional)

In Chapter 2, a central receiver CSP plant has been chosen for the analysis. In a central receiver CSP plant, the concentrator consists of numerous heliostats focusing the sunlight onto a specific area of the tower, which is called the receiver. A heat transfer fluid gets heated by the radiation on the receiver and is used to run the turbine in the power block. The third component of a CSP plant is the power block, which is usually a simple or a modified Rankin cycle consisting of following main parts (Cengel et al., 2011):

- Pump
- Boiler
- Turbines
- Condenser

Each component will be discussed in detail in the following sections. In the case of central receiver CSP plants, if the plant does not have a storage system, heat flux inside the receiver will turn water into steam. On the other hand, if the plant has a storage system, then water will be heated into steam using heat exchangers with the storage medium.

In order to integrate the CFB reactor designed in the last chapter, it is most economical to use one reactor to perform both the charging reaction during the day and the discharging process during the night. Unfortunately, this idea could not be implemented because in the charging process (endothermic reaction) more energy needs to be supplied to the reaction in order to form CaO as will be shown below.

4.1 The Endothermic Reaction

The endothermic reaction within the charging process introduces heat to convert $Ca(OH)_2$ into CaO and H_2O. The heat needed for the reaction is supplied by superheated steam, which is coming from the tower where it was generated by the heat flux in the receiver. The superheated steam is specified to be at 560 C and 100 kPa absolute (as discussed in Chapter 2) and the endothermic reaction becomes:

$$Ca(OH)_{2(s)} + H_2O_{(g)} \longrightarrow CaO_{(s)} + 2\ H_2O$$

The temperature of the H_2O in the products will be reduced, and a First Law analysis is applied to estimate the temperature. The First Law of Thermodynamics is simply an application of the conservation of energy principle and it can be expressed for steady flow systems as (Cengel, 2011):

$$Q - W = H_p - H_R$$

Where: Q is the heat added to the system

W is the work done by the system

H is the enthalpy for the products (p), and the reactants (r).

A control volume is set around the riser and since there is no work done by or on the system, W is to be equal to zero. Also, since the reaction is endothermic, heat must be supplied through the reactor. Therefore, the heat added to the system is equal to the enthalpy of products minus the enthalpy of the reactants. The enthalpy of a chemical component is expressed as the summation of the enthalpy of a component at a standard reference state (25 C and 1 atm), plus and the sensible enthalpy of the component relative to the standard reference (Cengel, et al., 2011).

$$\text{Enthalpy} = \bar{h}_f^o + (\bar{h} - \bar{h}^o) \quad \text{(kJ/kmol)}$$

Where $\bar{h}_f^o$ is the enthalpy of formation at 25 C and 1 atm.

$\bar{h}$ is the sensible enthalpy at a specified state.

$\bar{h}^o$ is the sensible enthalpy at the reference state.

The enthalpy of formation and the difference in sensible enthalpy for each species in the products and the reactants are shown in Table 17. After finding the enthalpy of each species, it is multiplied by the number of kmoles. Then the enthalpy of the products/reactants is equal to the summation of the enthalpy over all the species.

Table 17: Finding the enthalpy of reactants and products

T (C)	T(K)	Species	kmole	$\bar{h}_f^o$	$\bar{h} - \bar{h}^o$	n($\bar{h}_f^o$+$\bar{h} - \bar{h}^o$)
400	673	$Ca(OH)_2$	1	-986,090*	38,158	-947,932
560	833	H_2O	1	-241,820	2,427	-239,393
500	773	CaO	1	-635,090*	33,142	-601,948
500	773	H_2O	2	-241,820	16,837	-449,966

* Values are taken from JANAF tables (Chase, 1998).

H_2O is assumed to behave as an ideal gas and as a result its enthalpy of formation is taken from ideal-gas properties of H_2O tables (Cengel et al., 2011). In the table, the sensible enthalpy for calcium hydroxide, calcium oxide, and H_2O the sensible enthalpy is derived from the following integration (Cengel et al., 2011):

$$\bar{h} - \bar{h}^o = \int_{298}^{T} C_p dT$$

Where C_p is the specific heat constant

T is temperature

The specific heat constant for CaO, $Ca(OH)_2$, and H_2O can be expressed as a function of T as (Cengel, 2011):

$$\frac{C_p}{R} = A + BT + D\,T^{-2}$$

where R is the gas constant (R= 8.314 kJ/kmol-K)

The values for A, B and D for CaO, $Ca(OH)_2$, and H_2O are shown in the following table. Multiplying by the gas constant and integrating to find the sensible enthalpy, the following equations are found:

$Ca(OH)_2$: $\bar{h} - \bar{h}^o = 79.8\,T + 0.0226\,T^2 - 25{,}784 = 38{,}158$ kJ/kmol

CaO: $\bar{h} - \bar{h}^o = 50.75\,T + 0.0184\,T^2 + \frac{8.7E5}{T} - 18{,}208 = 33{,}142$ kJ/kmol

H_2O: $\bar{h} - \bar{h}^o = 28.85\,T + 0.006\,T^2 - \frac{10^5}{T} - 8{,}792 = 16{,}837$ kJ/kmol

Table 18: Specific heat constants for CaO, $Ca(OH)_2$, and H_2O (Spencer, 1948)

Species	A	10^3 B	10^{-5} D
CaO	6.104	0.443	-1.047
$Ca(OH)_2$	9.957	5.435	--
H_2O	3.470	1.450	0.121

The amount of heat that needs to be added is found to be 135,418 kJ/kmole. In similar situations where heat needs to be added to a system, fossil fuels would be a good medium to use. However, one of the main reasons to build a CSP plant is to decrease the production of global warming gasses generated from burning fossil fuels.

The proposed heat source is solar radiation, which is facilitated by integrating the fluidized bed reactor as part of the tower. The outside surface of the bed will be covered by a layer that is conductive to receiving solar radiation. Fins will be extended from the conduction layer into the fluidized bed in order to increase the heat flow rate into the riser. The charging reactor will not be lined with refractory as the goal is to promote heat transfer. Alternatively, during the exothermic reaction in the discharging process, heat loss must be minimized, so the reactor uses an insulating layer of refractory on the inner walls of the reactor. Therefore, two separate reactors must be used: one for the endothermic reaction with fins extended from the conduction layer, and the other is for the exothermic reaction with an insulating layer. The exothermic reactor will not be on the tower, but instead will be on the ground near the power block. A detailed description is provided below for the integration of the charging process into the cycle during the day, and the discharging process during the night.

4.2 Charging Process

4.2.1 Power Cycle

The charging process starts at the pump where water at atmospheric pressure is pressurized to 12.5 MPa absolute, as shown in step 1 of Figure 8. The pressurized water enters the tower where it is boiled and superheated to 550 C. Superheated steam leaves the tower toward the turbine (step 2). Since not all the steam entering

the turbine is needed for the thermochemical reaction in the reactor as will be shown later in this section, the needed amount of steam is withdrawn from the turbine at an intermediate pressure of 100 kPa absolute, and the rest is left to exit the turbine at 10 kPa absolute. At 100 kPa absolute, a mixture of liquid and steam is leaving the turbine at 100 C. The mixture heads back toward the tower but this time it enters the reactor (step 3). While the rest that is leaving at 10 kPa absolute is directed to the 10 kPa absolute condenser (step 3'). The endothermic reaction will happen inside the reactor with the help of the added heat using the fins. Calcium oxide and H_2O will be leaving the reactor each second. The hot CaO will be stored in an insulated storage. The H_2O will be sent to the 100 kPa absolute condenser (step 5). When leaving the condenser, the steam will be turned onto water, the amount generated by the reaction will be sent toward a H_2O storage while the rest will head toward the pump for the cycle to start again (steps 6 and 6'). At the end of the endothermic reaction CaO will be produced and stored to be used at night (step 7).

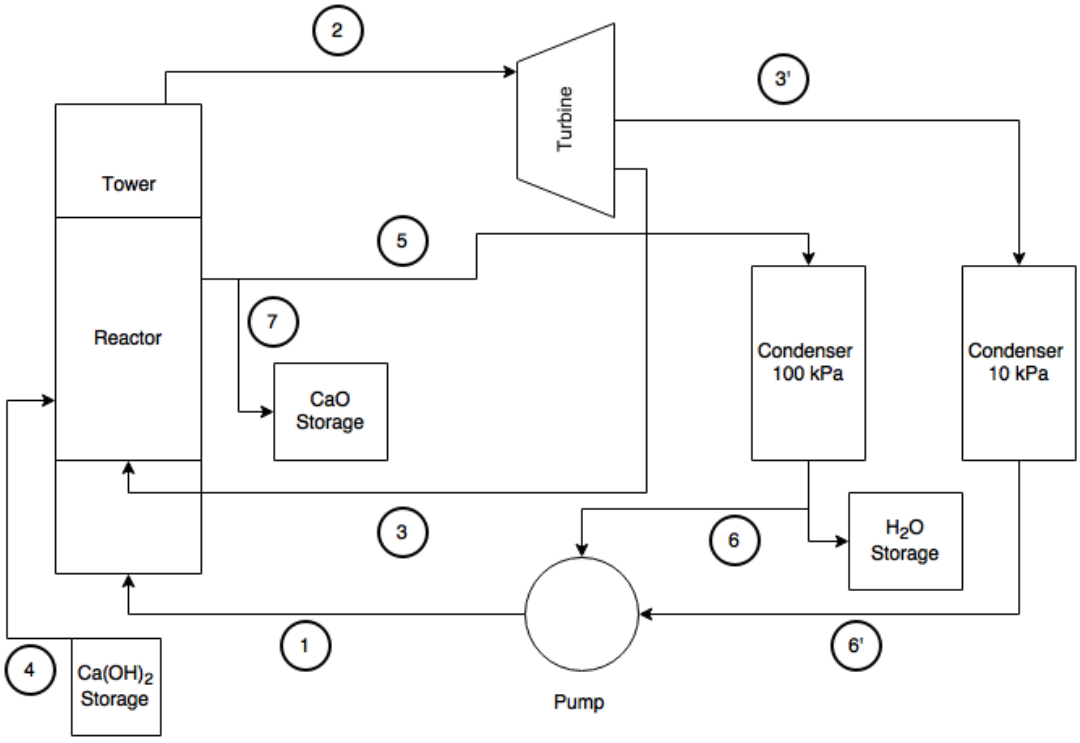

Figure 8: Charging process Layout.

As will be shown in the discharging process section, 4.3 kmoles/s of CaO is needed for the reaction during the night, which means the same amount of kmoles/s of

$Ca(OH)_2$ needs to dehydrate during the day. From the endothermic reaction, the proportionality between the amount of kmoles of $Ca(OH)_2$ and H_2O in the reactants is 1:1. This means, if 4.3 kmoles/s of $Ca(OH)_2$ is used for the reaction, 4.3 kmoles/s of H_2O is needed as well:

$$4.3\ Ca(OH)_{2(s)} + 4.3\ H_2O_{(g)} \longrightarrow 4.3\ CaO_{(s)} + 8.6\ H_2O_{(s)}$$

To produce 100 MW_e from the turbine, the enthalpies at steps 2, 3 and 3', and the mass flow rate for steam must be known. At step 2, steam is entering at 550 C and 12.5 MPa, that leads to an enthalpy h_2= 3476.5 kJ/kg and entropy s_2= 6.6317 kJ/kg-K (Cengel, 2011). At step 3, flow must leave at 100 kPa absolute, which is a saturated mixture. Assuming an isentropic case, s_3=s_2, and that leads to $h_{3,s}$= 2404.11 kJ/kg with steam quality x= 88% (Cengel, 2011). At step 3', flow leaves the turbine at 10 kPa absolute, $h_{3',s}$= 2100.1 kg/kJ, with $s_{3'}$=s_2. The isentropic work out of the turbine then would be

$$w_s = y\ h_2 - (1-y)(h_{3,s} + h_{3,s'})$$

$$y = \frac{\dot{m}_3}{\dot{m}_2}$$

As a result, w_s= 7980.62 y -4504.12.

The isentropic case is an ideal situation, but the actual work out of the turbine (w_a) with the assumption that the turbine has an isentropic efficiency of 90% will be:

$$w_a = \eta_T\ w_s = (0.90)(7980.62\ \text{y} - 4504.12) = 7182.56y - 4053.71\ kJ/kg$$

The steam mass flow rate then can be calculated by the following equation:

$$\dot{m}_2 = \frac{\dot{m}_3}{y} = \frac{\dot{W}}{w_a} = \frac{100{,}000\ kW}{7182.56y - 4053.71 kJ/kg}$$

Knowing $\dot{m}_3$= 4.3 kmoles/s= 77.4 kg/s, then y and $\dot{m}_2$:

$$\text{y= } 68.82\%$$

$$\dot{m}_2 = 112.47\ \text{kg/s}$$

The amount of heat addition required is specified via the use of the First Law of Thermodynamics:

$$Q = H_P - H_R$$

By specifying the products and the reactants temperatures, the enthalpies can be found and then the amount of heat. For reactants, H_2O is entering at 100 C, and because the $Ca(OH)_2$ was produced at 400 C and stored in an insulated tanks, it will enter the reactor at 400 C. Both the CaO and steam products are specified to leave at 500 C. Table 17 shows the enthalpy of formation, sensible enthalpy and the enthalpy of products and reactants. From the table, the amount of heat supplied is 135,418 kJ/kmole of $Ca(OH)_2$. Since 4.3 kmoles/s of $Ca(OH)_2$ will be entering, the total of heat flux needed is Q=582,297 kW.

4.2.2 Fins

To improve the flow of heat from the outside surface to the contents of the fluidized bed, the decision is made to use extended surfaces between the wall of the bed and the interior cavity. The use of fins extending inward from the outside wall appears to be the best option. The exterior conduction layer is chosen to be C 1100 copper alloy for its high thermal conductivity (k= 388 w/m-K) and the conduction layer is assumed to be at 800 C. This temperature is achieved by focusing some of the heliostats on the receiving surface of the reactor while the rest will be focused on the tower receiver where water is heated to become superheated steam.

The heat transfer from the fins to the interior flow is primarily convective heat transfer where the heat transfer from one fin is governed by the following equation (Incropera, 2007):

$$Q = \sqrt{hPkA_c}\theta_b$$

Where h= Convictive heat transfer coefficient

P= Fin perimeter

k= Thermal conductivity

A_c= Fin cross-sectional area

θ_b= Temperature of the fin base (T_b) − Temperature of the flow (T_∞)

The fins are assumed to be very long, which means the temperature of the fin tip is equal to the temperature of the flow. Since the flow is carrying particles with it, the convictive heat transfer coefficient (h) will be higher than that for a corresponding gas flow. Figure 9 below shows for particles in the range of 200 μm, h is equal to an

average of 400 W/m^2-K (Basu, 2015). Because of mixing process between solid particles and gas inside the reactor, the temperature is assumed to be uniform at 500 C. As a result, the temperature difference (θ_b) is equal to 300 C. Knowing how much heat can be transferred from one fin and the total amount of heat needed, the total number of fins required can be calculated.

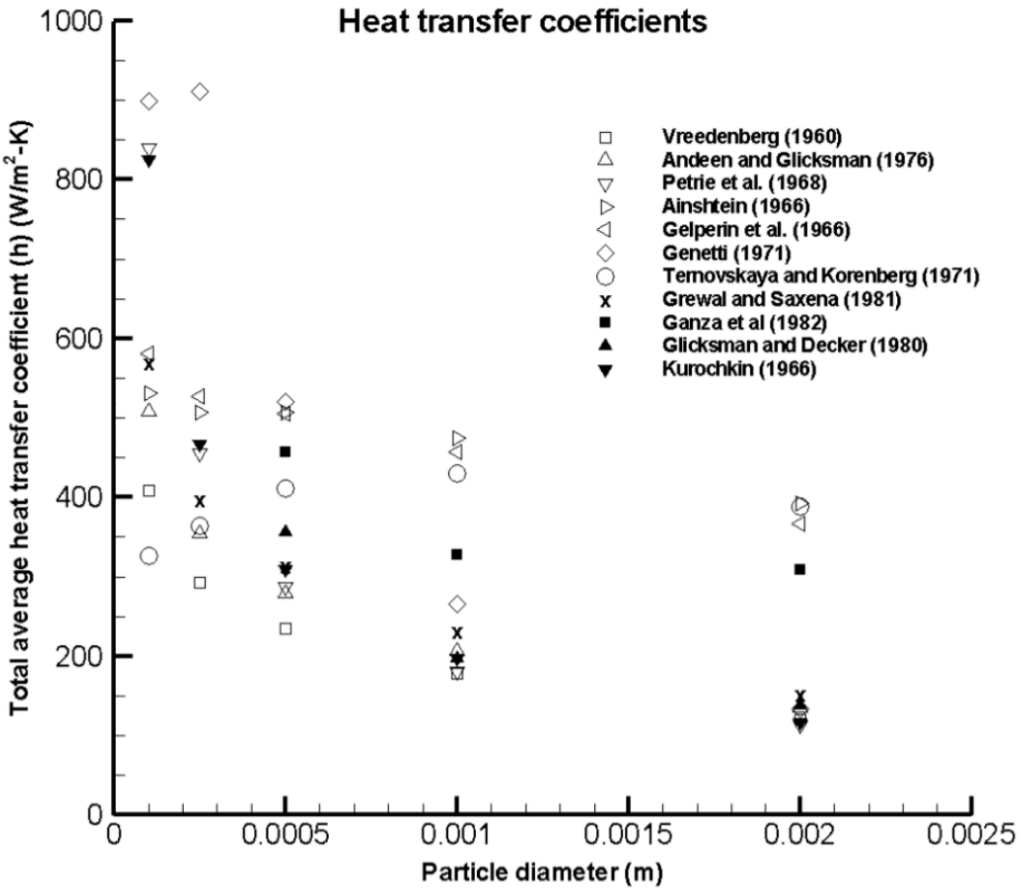

Figure 9: Experimental correlations for heat transfer coefficient for fluidized beds

For fins with circular cross section, $P = \pi D,\ A_c = \pi D^2/4$, where D is the fin diameter, Q depends on the diameter. The diameter of the fins has been varied from 8 mm to 70 mm in order to find the diameter with the optimal thermal performance and the lowest cost. The thermal performance can be optimized by increasing the ratio of spacing between fins over the diameter (S/D), and the ratio of the length over the diameter (L/D) (Brigham et al., 1984). The S/D and L/D ratios were found to be the highest for a diameter of 8 mm. Following the assumption that the fins are treated to be very long fins,

the length must be equal to or greater than a specified value, and this value is estimated by the equation below (Incropera, 2007):

$$L \geq L_{\infty} = 2.65 \left(\frac{kA_c}{hP}\right)^{1/2}$$

For 8-mm diameter, L ≥ 11.67 cm, L/D = 14.6 and S/D = 0.5875. Table 19 shows various values of diameter and their corresponding thermal performance ratios.

Table 19: Multiple fin diameters and their corresponding total cost

D (mm)	L (m)	S/D	L/D	Number of fins	Total Cost
8	0.117	0.5875	14.6	4.38E+06	$1,830,000
10	0.130	0.5	13.0	3.14E+06	$2,290,000
20	0.185	0.25	9.23	1.11E+06	$4,570,000
30	0.226	0.13	7.53	6.04E+05	$6,860,000

As shown in the table above, as the diameter increases, the thermal performance ratios decrease and the total cost increases. The total cost is found by knowing the total mass of the fins and the fact that the cost of 1 kg of C 1100 copper alloy is 8 dollars (C1100 copper rod price, 2016). Appendix I shows the full list of diameters and the calculations for the performance ratios, number of required fins, and the total cost for all the considered diameters.

4.3 Discharging process

After designing the reactor that is going to be used for the charging process, calcium oxide will be produced all day long and stored in an insulated tank. When the sun sets, the exothermic reaction for the discharging process will start, where the exothermic reaction is:

$$4.3\ CaO_{(s)} + 4.3\ H_2O_{(g)} \longrightarrow 4.3\ Ca(OH)_{2(s)}$$

As discussed earlier, the reaction has to take place in a separate reactor since the inside of the reactor must be insulated. As shown in Figure 10, water coming from H_2O storage and the 10 kPa condenser will enter the pump to be pressurized to 12.5 MPa (step 1 and 1'). Then it will head toward the reactor where it flows inside the water-walls (pressurized) (step 2). Because of the exothermic reaction inside the reactor, heat will be radiated toward the water-walls. The generated heat will be

used to heat up the liquid water to a superheated steam. Superheated steam will leave the reactor toward the turbines to generate electricity (step 3). At an intermediate pressure of 100 kPa absolute, most of the steam will be pulled out of the turbine as a saturated mixture, while the rest will come out of the turbine at 10 kPa absolute and it will be directed toward the 10 kPa absolute condenser (step 4'). Saturated mixture leaving the turbine at 100 kPa absolute will enter the reactor inside another set of water-walls (non-pressurized) (step 4). It will also grasp some of the heat generated from the exothermic reaction to turn to steam. After leaving the water walls, steam will enter to the reactor (step 5) to react with CaO coming from the storage (step 6). In the reaction, $Ca(OH)_2$ will be created and it will be sent to an insulated tank to be used during the day for the endothermic reaction (step 7), then the cycle will repeat itself starting at step 1 and 1' again.

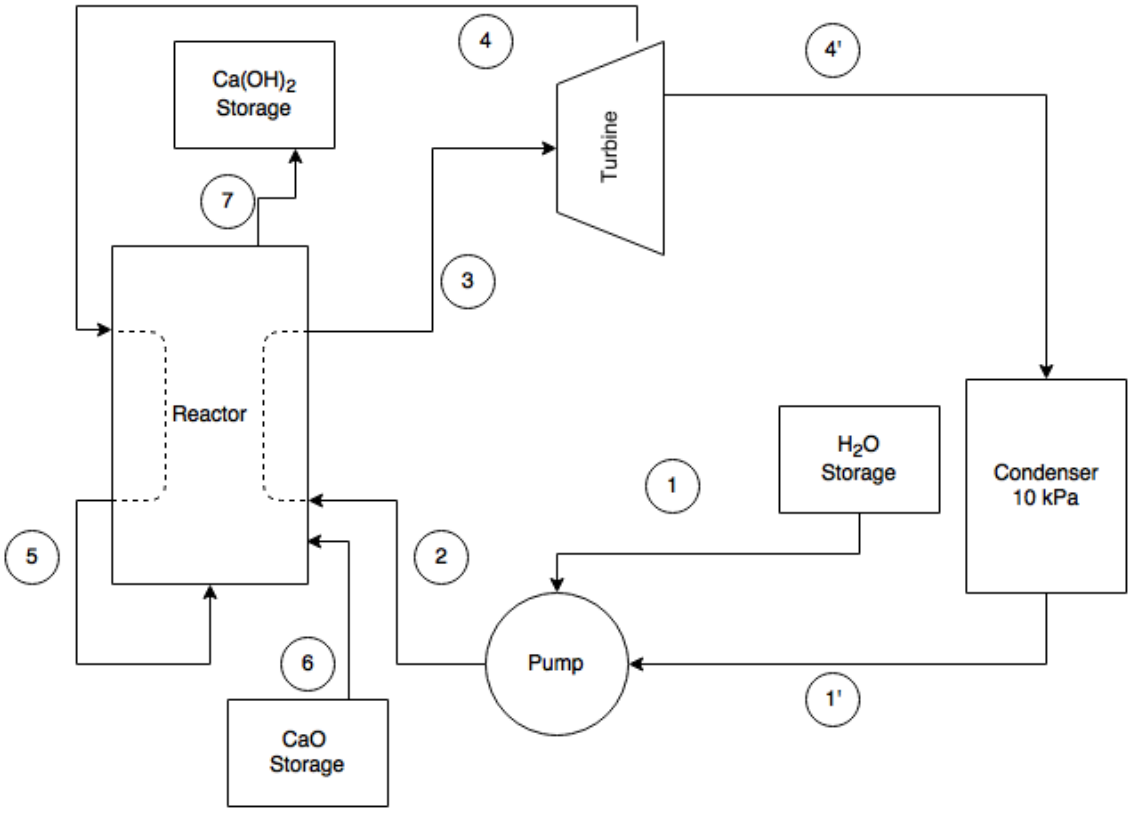

Figure 10: Discharging process layout

The mass flow rate needed to produce 100 MW_e of power is calculated the same way as in the charging process. At step 3, superheated steam will enter the turbine

at 400 C and 12.5 MPa absolute, and the amount needed for the exothermic reaction ($\dot{m}_4$=77.4 kg/s as shown below) is going to leave at 100 kPa absolute (step 4). The rest of steam will leave the turbine at 10 kPa absolute toward the 10 kPa absolute condenser (step 4'). The isentropic work out of the turbine is:

$$w_s = y\ h_3 - (1-y)(h_{4,s} + h_{4,s'})$$

$$y{=}m4/m3$$

With the assumption that the isentropic efficiency of the turbine being 90%, the actual work becomes, w_a= 6432.24y- 3687.24 kJ/kg. Therefore, y= 71.86% and the mass flow rate is

$$\dot{m}_3 = \frac{\dot{W}}{w_a} = 107.71\ kg/s$$

This is the amount of water/steam that needs to go through steps 2 and 3, but the amount going through steps 4 and 5 is different and depends on how much heat is needed to be produced inside the reactor. The amount of heat produced inside the reactor needs to be enough to cover the heat needed for water walls between steps 2 and 3, and steps 4 and 5. Also, there is an assumption that no more than 2% of generated heat is going to escape through the refractory walls. One kmole of CaO reacting with one kmole of H_2O can produce 109,182 kJ/kmole of CaO. Therefore, a 4.3 kmole/s reaction will produce 469,482 kW. As will be shown in the next section, the amount of heat needed for water-walls is 395,122 kW and the 2% escaping through the refractory is 7,902kW.

4.3.1 Water-walls

Heat is generated inside the reactor by the exothermic reaction, and this heat is picked up by the colder flow inside the water-walls. Water-walls are pipes carrying water/steam that gets heated by an external heat source. For water to be heated to superheated steam it goes through 3 steps. The water-walls consists of a set of pipes leaves a water drum toward steam drum, then another set leaves the steam drum, passes through the heater, and then is directed to the turbine (Woodruff et al., 2005). The first set is the economizer and the boiler, while the second set is the superheater.

For water-walls between steps 3 and 4, a compressed liquid water at 12.5 MPa absolute enters the reactor at an enthalpy of h= 171.06 kJ/kg, and leaves as superheated steam at 400 C and 12.5 MPa absolute at an enthalpy of h=3040 kJ/kg. The amount of heat needs to be added to the flow from the exothermic reaction is:

$$q = \dot{m}\,\Delta h = (107.71\ kg/s)\ (3040 - 171.06) kJ/kg = 309{,}014\ kW$$

On the other hand, the water-walls between step 5 and 6 are at 100 kPa absolute and have a 4.3 kmoles of H_2O running through them, which is equal to 77.4 kg of H_2O. Saturated mixture enters the pipes at 100 kPa absolute with an enthalpy of h= 2271.14 kJ/kg, while superheated steam leaves the water-walls then enters the reactor at 450 C and 100 kPa absolute with an enthalpy of h= 3383.65 kJ/kg. As a result, the amount of heat needed is:

$$q = \dot{m}\,\Delta h = (77.4\ kg/s)\ (3383.65 - 2271.14) kJ/kg = 86{,}108\ kW$$

With the amount of heat transfer being known, the surface area of water-walls is specified. The surface area consists of the number of pipes in the water walls, the length of pipes and their diameter. To relate the number of pipes to the total length of the pipes a heat transfer analysis is carried out. The heat transfer analysis below is applicable for both the economizer and the superheater since both have a single-phase fluid running inside them, while different type of analysis is carried out for the boiler because of the two-phase fluid inside it.

4.3.2 Heat transfer Analysis

4.3.2.1 Economizer and Superheater

Heat is transferred to the flow inside the pipes via three steps: first is through convection from the hot bed to the outer wall of the pipe. The second step is from the outer wall of the pipe to the inner through the thickness of the pipe by conduction. Third step is by convection form the inner wall of the pipe to the flow inside.

$$q = \frac{\Delta T_{lm}}{R}$$

where q is heat transfer

ΔT_{lm} is the log mean difference in temperature

R is the thermal resistance

The mean log difference in temperature is used because the flow inside the pipes does not have a uniform temperature. Therefore, to specify the temperature difference to use for the heat transfer, the inlet, outlet and the heating temperatures are all used as flows (Incropera, 2007):

$$\Delta T_{lm} = \frac{\Delta T_o - \Delta T_i}{\ln\left({}^{\Delta T_o}/_{\Delta T_i}\right)}$$

$$\Delta T_o = T_{\infty,o} - T_o$$

$$\Delta T_i = T_{\infty,o} - T_i$$

where $T_{\infty,o}$ is the temperature of the bed (heating temperature)

T_o is the outlet temperature (i.e. saturated liquid temperature for the economizer)

T_i is the inlet temperature (i.e. saturated vapor temperature for the superheater)

The thermal resistance is equal to the reciprocal of the overall heat transfer coefficient (U) multiplied by the total surface area (A_T):

$$R = \frac{1}{UA_T}$$

The total surface area is equal to the surface area of one pipe (A) multiplied by the number of pipes (n), which leads to:

$$q = n\,(UA)\,\Delta T_{lm}$$

Using the outer surface area of the pipes and dividing by the length of each pipe:

$$\frac{q}{L} = n\left(\frac{U_o A_o}{L}\right)\Delta T_{lm}$$

$$\left(\frac{UA}{L}\right) = \frac{1}{\frac{1}{2\pi r_o h_o} + \frac{\ln\left({}^{r_o}/_{r_i}\right)}{2\pi k} + \frac{1}{2\pi r_i h_i}}$$

The three terms in the denominator are for convective heat transfer from the bed to the outer wall, the conductive heat transfer through the thickness, and the convective heat transfer from the inner wall to the inside flow, respectively.

The most commonly used material for the pipes in water-walls is carbon steel which has a thermal conductivity of 32.9 w/m-K at 455 C (Woodruff et al. 2005). The outer

heat transfer coefficient (h_o) is already known (400 w/m^2-K). The inside heat transfer coefficient (h_i) depends on the inside diameter as the following equation (Incropera, 2007):

$$h_i = \frac{Nu_D D}{k} = \frac{0.023\ Re^{4/5} Pr^{0.4}\ D}{k}$$

$$Re = \frac{4\ (\frac{\dot{m}}{n})}{\pi D \mu}$$

Where Nu_D: Nussult number D: inside diameter

k: thermal conductivity Re: Reynolds's number

Pr: Prandtl number $\dot{m}$: mass flow rate

n: number of pipes μ: dynamic viscosity

The typical outer diameter for economizer and boiler pipes ranges from 30 mm to 80 mm (Teir, 2003), while for the superheater pipes it ranges from 50 mm to 80 mm. From ASME/ANSI B36.10 Welded and Seamless Wrought Steel Pipe standard (2004), there are five pipe diameters that fall within the specified range as shown in table 20. The thickness and the inner diameter are specified using the schedule number, which is:

$$Sch. = 1000\ \frac{P}{S} = 1000\ \frac{(12.5\ MPa)}{(80\ MPa)} = 156$$

Where P is the service pressure and S is the yield strength at 455 C. Since there is no 156 schedule number, schedule 160 is used. With the diameter known, h_i can be found in terms of number of pipes.

Table 20: Outer diameter, inner diameter, and thickness for water-walls pipes

Outer diameter (m)	Thickness (m)	Inside diameter (m)
0.0334	0.00635	0.0207
0.0422	0.00635	0.0295
0.0483	0.00714	0.03402
0.0603	0.00874	0.04282
0.073	0.00953	0.05394

The heat transferred from the hot flow is the same as the heat accepted by the cold flow, which is equal to the mass flow rate multiplied by the difference in the enthalpy of the flow:

$$q = \frac{\dot{m}}{n}\,\Delta h$$

With the heat transfer known, the length of the pipes can be found as:

$$L = \frac{q}{n\left(\frac{U_o A_o}{L}\right)\Delta T_{lm}}$$

As a result, increasing the number of pipes decreases the length of pipe. The optimum lengths and number of pipes combination is the one that gives the smallest volume of thickness, which corresponds to lowest overall cost. Table 21 gives the optimal diameter, length and the corresponding volume for the economizer and superheater for the pressurized and non-pressurized water-walls. Appendix II shows a detailed analysis for all the different diameters, and the calculations for the optimal number of pipes, length and volume.

4.3.2.2 Boiler

The boiler has two-phase flow inside the water-walls, which means it needs a different heat transfer analysis. Here, the typical convection heat transfer coefficient for boiling water/steam mixture is around 100,000 w/m^2-K (Incropera, 2007), and as a result its effect is negligible in the heat transfer process. That is:

$$\left(\frac{UA}{L}\right) = \frac{1}{\frac{1}{2\pi r_o h_o} + \frac{\ln\left(r_o/r_i\right)}{2\pi k}}$$

The mean log temperature difference is not needed in this case because the inlet and the outlet temperature for the flow are the same. Therefore, the temperature difference between the hot bed and the inside flow is:

$$\Delta T = T_{\infty,o} - T_o$$

For example, the temperature difference in the non-pressurized boiler pipes is 455-100= 355 K. And since,

$$q = \frac{\Delta T}{R}$$

Therefore,

$$R = \frac{\Delta T}{q} = \frac{355\ (K)}{31.26\ (MW)} = 1.135 * 10^{-5}\ (K/W)$$

Since the water-walls extend from the water drum to the steam drum, the economizer and the boiler have the same pipe diameter. Therefore, it is assumed that the boiler in the pressurized and non-pressurized water-walls will have the same pipe diameter (D_o= 0.0422 m) and the same number of pipes (260).

$$R = \frac{1}{n\,L}\left[\frac{\ln\left({}^{r_o}/_{r_i}\right)}{2\pi k} + \frac{1}{2\pi r_o h_o}\right] = \frac{1}{L}[\,0.0205]$$

Resulting in the length of each pipe being 6.94 m. Table 21 summarizes the results for the water-walls pipes diameter, length and volume.

Table 21: Water-walls optimal diameter, length and volume.

Type		Q (MW)	Optimal diameter (m)	Number of pipes	Length of pipes (m)	Thickness volume (m^3)
Pressurized	Economizer	266	0.0422	260	15.10	2.81
	Boiler	125.2	0.0422	260	7.7	1.43
	Superheater	39.4	0.0603	180	6.35	1.62
Non-pressurized	Boiler	31.26	0.0422	260	6.94	1.29
	Superheater	54.8	0.0603	150	10.07	2.13

Designing the water-walls concludes the discharging process, which concludes the integration of the reactor in the power cycle. The functionality of the technology is not the only factor that determines its viability, one important other factor is the cost of the technology, which will be discussed in the next chapter.

Chapter 5: Economics and Policy

At this point a proposed thermal storage system has been specified. This chapter develops a cost analysis of the technology to evaluate its economic competitiveness.

5.1 Levelized Cost of Electricity (LCOE)

One way to compare different electricity generation technologies is through the use of Levelized Cost of Electricity (LCOE). LCOE takes into account the capital cost of the power plant, the fixed and variable operation and maintenance (O&M) cost, and performance and fuel cost (EIA, 2013). LCOE, which is usually presented as cents per kilowatt-hours (cents/kWh), can be used to compare different technologies (renewable and non-renewable) and compare different power plant sizes. LCOE does not take into account financing issues, discount issues, replacement or degradation costs (EIA, 2013).

5.1.2 Capital Cost

The capital cost parameter in LCOE consists of (EIA, 2013):

- Civil/structural material and installation such as site preparation
- Mechanical equipment supply and installation including major equipment such as boilers.
- Electrical instrumentation and controls (I&C) supply and installation
- Project indirect costs, fees and contingency including distributable labor and materials, construction management, and start-up and commissioning.
- Owner's costs including preliminary feasibility and engineering studies.

5.1.1 Operation and Maintenance (O&M) expenses:

O&M expenses consist of fixed and variable expenses. Fixed expenses are those which do not vary significantly with generation such as: personnel costs, and maintenance of structures and grounds. Some O&M expenses vary with the electricity generation rate such as consumable material and supplies, lubricants, and waste disposal expenses.

The table below gives the capital cost expenses for a 100 MW solar thermal power plant with no storage (i.e., the base system) (EIA, 2013). Since all the expenses are taken into consideration for all the components of the power plant, adding the additional expenses of the storage system to the base cost will give the

total cost for a 100 MW CSP plant with thermochemical TES system. The items that need to be added to the capital cost are related to the two reactors, such as the cost of the refractory and water-walls for the reactor in the discharging process, and the fins for the reactor in the charging process. This also includes the cost of the calcium hydroxide reagent, assuming it can tolerate 1095 cycles (3 years).

Table 22: Capital cost for a 100 MW solar tower power plant.

Capital Cost category	2012$
Civil structural Material and installation	50,414,000
Mechanical Equipment supply and Installation	270,340,000
Electrical/ I&C Supply and Installation	42,380,000
Project Indirects (1)	41,080,000
EPC Cost before Contingency and fee	404,214,000
Fee and Contingency	36,400,000
Total Project EPC	440,614,000
Owner Cost (excluding project finance)	66,092,000
Total Project Cost (excluding project finance)	506,706,000

(1) Includes engineering, distributable costs, scaffolding, construction management, and start-up.

As discussed in Chapter 4, since the amount of calcium hydroxide needed is 4.3 kmole/s and since the price of one ton of $Ca(OH)_2$ is $290 (Calcium hydroxide price, 2016), The cost of $Ca(OH)_2$ is:

$$\frac{4.3\ kmole\ Ca(OH)_2}{1\ s} * \frac{3600\ s}{1\ hr} * 12\ hr * \frac{74.093\ kg}{1\ kmole} * \frac{1\ ton}{1000\ kg} * \frac{\$290}{1\ ton} = \$3{,}710{,}000$$

This amount of $Ca(OH)_2$ is projected to last through three years of use. Assuming the power plant will be running for 30 years, a total of 10 purchases are needed. The total amount needed will cost 33 million of present worth (2012) dollars.

The number of fins in the charging process is related the amount of heat required to be added to the $Ca(OH)_2$. The total cost of fins as discussed in Section 5.2.2 is $1,830,000. From Table 20, the total volume for water walls is 9.28 m^3. Since the pipes will be made of carbon steel with a density of 7850 kg/m^3 and costs $750 per ton (Carbon steel price, 2016), the total cost for water walls is $54,600. The total cost of refractory is calculated in Table 15 to be $25,300. The cost of the CaO storage

unit, the $Ca(OH)_2$ storage unit and the H_2O storage unit is estimated to be $29,400. The cost comes from the carbon steel enclosure. The same calculations are made for the riser and downcomer in the two reactors, the cost ends up being $139,000. Adding all the expenses, the total capital cost is $542,200,000.

On the other hand, fixed and variable O&M expenses should not change from the model. The fixed O&M expenses is $67.26/kW-year, while variable O&M expenses are $0/MWh (EIA, 2013). To calculate the LCOE the following formula is used:

$$LCOE = \{\frac{capital\ cost * capital\ recovery\ factor\ (CRF) + fixed\ O\&M\ cost}{8760 * capacity\ factor}\} + variable\ O\&M\ cost$$

The capital cost is measured in dollars per installed kilowatt ($/kW), while fixed O&M cost in $/kW-yr. The capital recovery factor (CRF) is a fraction and is calculated as:

$$CRF = \frac{i(1+i)^n}{(1+i)^n - 1}$$

where i is the discount rate which assumed to be 7% and n is the number of annuities received, which assumed to be 30 years (EIA, 2013). This values for i and n lead to a CRF value of 8%.

The capacity factor for this system is not known yet, however, it can be estimated. The capacity factor for a system without storage is around 30% (EIA, 2013). Assuming the system will work at night the same way it is working during the day, then the capacity factor is estimated to remain around 30%.

$$LCOE = \frac{(5422.0\ \$/kW\ ) * (0.08) + (67.26\ \$/kW - yr)}{(8760\ hr * 0.3)} = 19\ cents/kWh$$

Comparing this value to the median for CSP plants, which is 18 cents/kWh (EIA, 2013) the LCOE with the thermochemical reactor is one cent higher. The increase is due to the capital cost of the reactor and storage material. Table 23 compares their median LCOE values for different technologies.

Table 23: LCOE for different renewable and non-renewable technologies.

Technology	LCOE (cents/kWh)	Technology	LCOE (cents/kWh)
Wind, Onshore	7	Biopower	7
Wind, Offshore	13	Distributed generation	11
Solar, PV	29	Fuel Cell	11
CSP	18	Natural Gas Combined Cycle	5
Geothermal, Hydrothermal	6	Natural Gas Combustion Turbine	9
Enhanced Geothermal system (EGS)	9	Coal, Pulverized Coal, Scrubbed	6
Small Hydropower	10	Coal, Integrated Gasofication Combined Cycle	8
Hydropower	6	Nuclear	8

As can be seen from the table, the LCOE obtained from using the thermochemical system is not very competitive with non-renewable enrgy sources such as coal or nuclear. However, it is comparable to solar PV and CSP. The main advantage of the system is the ability to produce electricity contiounsly for 24 hours, which cannot be done by other renewable sources. This 24 hours electricty production solves one of the main problems with renewable energy sources which is the intermittency.

5.2 Policy

The barriers in the way of implementation of renewable energy can be classified as science related barriers and socio-political barriers (Tweidell et al., 2009). The science related barriers represent 25% percent of the problem, while 75% percent is because of the socio-political barriers (Tweidell et al., 2009). There are multiple factors that should be considered because of its influence on energy supply policy such as:

- Security of supply

  Depending on fossil fuels as the main source of energy when supply is scarce or constrained raises a great risk in case of any international disruption at the production sources. Therefore, the use of renewable energy resources can solve the problem of the energy supply because every country has its own renewable energy source that should be used as a major component of energy production. Moreover, the use of renewable energy sources prevent the depletion of the finite resources.
- Diversity of supply

  The dependence on one source as the major component of the energy supply has a high risk, while the diversification increases the security of the energy supply. The different types of renewable energy can clearly provide this diversity and increase security.
- Economics of supply:

  The prices of the various forms of energy are heavily influenced by materials cost, taxes, subsidies, monopoly influences and supplier profits (Tweidell et al., 2009). Renewable energy utilizes freely available environmental resources such as sunshine and wind. This generally means the capital cost dominates the overall economics. The application of subsidies and/or taxes can be used to reflect the overall environmental cost of placing CO_2 in the atmosphere, and this can have a dominant effect on the competitiveness of renewable technologies.
- Health and safety:

  The negative impacts of fossil fuels on humans and the environment cannot be neglected. In general, renewable energy technologies significantly reduce these impacts. The exceptions are noise, potential damage to wildlife, and emissions associated with the manufacturing of the systems (Twidell et al., 2009).

All of these factors have motivated new legislation and policies that promote renewable energy by making it more competitive with fossil fuels. One example is

the introduction of a CO_2 cap-and-trade system where a limit on CO_2 emissions is set, and companies are permitted to trade the unused portion to other companies that uses more than the limit. This will provide companies with profit incentives and accelerate the reduction of harmful emissions. This will also reduce the gap in cost between energy technologies using fossil fuels and those using renewables because now the cost of the emissions of CO_2 as byproduct is counted. This will tend to reduce CO_2 production. The CO_2 cap-and-trade system could be accompanied with the introducing of a carbon tax. A carbon tax can be defined as a tax based on greenhouse gas (GHG) emissions produced from the burning of fossil fuels (Palmer et al., 2010) and in which a specified price is paid for each ton of GHG emitted. Also, policymakers should increase the investment in research and development (R&D) in the renewable energy area. If successful, R&D can reduce the overall cost of renewable energy by increasing production efficiency or reducing the capital cost (Palmer et al., 2010). Also, many of the highest-valued renewable energy sites in the US are in remote areas with no transmission lines available to connect the sources to the electrical power grid (Palmer et al., 2010). Subsidizing the expansion of transmission lines will significantly improve the competitiveness of renewable energy resources and improve their market share.

Chapter 6: Conclusion and Recommendations

The burning of fossil fuels as a source of energy (1) depletes a non-renewable energy source, and (2) contributes greenhouse gas emissions to the atmosphere. Power generation using renewable resources significantly reduce both global warming emissions and the depletion of natural resources.

One problem with many renewable energy sources is that they are intermittent. For solar systems, thermal energy storage has been suggested as one means of addressing this problem. Thermochemical TES using the $Ca(OH)_2/CaO$ reaction is estimated to maintain the same capacity factor (30%) achieved by CSP plants with no storage system, accompanied with an increase in the LCOE median value from 18 cents/kWh to 19 cents/kWh. This has been accomplished by designing two circulating fluidized bed reactors and integrating them with a power generation cycle in a central receiver CSP plant. This design provides electricity for 24 hours, which means that the design can overcome the intermittency problem faced by renewable energy sources. The total capital cost of the plant has been found to be $542,200,000, while the fixed O&M is $67.26/kW-year.

The two reactors have a height of 37.5 m and a diameter of 7.2 m for the endothermic reactor and 8 m for the exothermic reactor. During the day, $Ca(OH)_2$ disassociates to CaO and steam via an endothermic reaction that is fueled by solar radiation. The reactor is placed in the tower where some of the heliostats are focused on its outer receiving layer. From the inside there is a conduction layer with fins extended to supply the extra heat needed for the reaction to take place happen. The other reactor is for the exothermic reaction in which CaO is reacted with steam to produce $Ca(OH)_2$ and release the energy stored during the day. This reactor is insulated with refractory to reduce heat loss. The heat released is used to heat cold water that flows inside water-walls and and generate superheated steam.

If the results acquired in this paper could be applied to utility scale CSP plants, the competitiveness CSP plants will significantly increase and the mismatch between power demand and supply will be decreased if not eliminated. Therefore, building a lab scale unit is recommended to check if the results of this paper can be acquired in reality.

Appendix I: Fin design:

The design of fins is governed by the following equation:

$$Q = \sqrt{hPkA_c}\theta_b$$

Where Q is the heat transfer from the fin

h= Convictive heat transfer coefficient

P= Fin perimeter

k= Thermal conductivity

A_c= Fin cross-sectional area

θ_b= Temperature of the fin base (T_b) − Temperature of the flow (T_∞)

To find an optimal fin diameter, the diameters are varied from 8 mm to 70 mm. The convective heat transfer coefficient is estimated to be 400 W/m²-K. The material used for the fins is C 1100 copper alloy, which has a high thermal conductivity coefficient of 388 W/m-K. The perimeter and the cross sectional area are functions of the fin diameter as show in the following equations:

$$P = \pi D$$

$$A_c = \frac{\pi D^2}{4}$$

The temperature difference between the fin base and the flow is 300 K because the fins base is assumed to be at 800 C and the flow is set to be at 500 C. The total amount of heat that needs to be added is 582,297 kW.

Sample calculation:

For a diameter of 8 mm:

$$P = \pi D = \pi \left(\frac{8}{1000}\right) m = 0.0251\, m$$

$$A_c = \frac{\pi D^2}{4} = \frac{\pi \left(\frac{8}{1000}\right)^2}{4} = 5.026x\ 10^{-5}\, m^2$$

Therefore, the amount of heat transfer from one fin is:

$$Q = \sqrt{hPkA_c}\theta_b = \sqrt{(400\frac{W}{m^2K})(0.0251\ m)(388\frac{W}{m\ K})(5.026x10^{-5}m^2)}\ (300\ K)$$

$$= 132.8\ W\ = 0.1328\ kW$$

The total number of fins required is

$$number\ of\ Fins = \frac{Total\ heat\ required}{heat\ per\ fin} = \frac{582{,}297\ kW}{0.1328\ kW} = 4.38\ x10^6\ fin$$

The length of each fin follows the assumption that the fins are long enough that the temperature of the fin's tip is equal to the temperature of the flow. Therefore, the length of is equal to or longer than:

$$L \geq\ L_\infty = 2.65\sqrt{\frac{kA_c}{hP}} = 2.65\sqrt{\frac{\left(388\frac{W}{m\ K}\right)(5.026x10^{-5}m^2)}{\left(400\frac{W}{m^2K}\right)(0.0251m)}} = 0.1167\ m$$

Therefore, the volume for each fin is

$$V =\ A_c\ L = (5.026x10^{-5}m^2)(0.1167m) = 5.87x10^{-6}m^3$$

From the volume and the density of C 1100 copper alloy, the mass is calculated:

$$m = V\ \rho = (5.87x10^{-6}m^3)\left(8890\frac{kg}{m^3}\right) = 0.05215\ kg$$

The total cost of the fins is calculated by multiplying the mass of one fin by the total number of fin by the cost of one kg of the fin material:

$$Total\ cost = (0.05215\ kg)(4.38x10^6 fin)\left(\ 8\frac{\$}{kg}\right) = \$\ 1{,}830{,}000$$

The table below gives the calculations for diameters from 8 mm to 70 mm.

Table 1: Number of fins, volume and total cost of fins as function of diameter.

D(m)	A_c (m^2)	P(m)	Q(kW)	Number of fins	L(m)	V(m^3)	Mass(kg)	Total cost ($)
0.008	5.03E-05	2.51E-02	1.33E-01	4.38E+06	1.17E-01	5.87E-06	5.22E-02	1.83E+06
0.009	6.36E-05	2.83E-02	1.59E-01	3.67E+06	1.24E-01	7.88E-06	7.00E-02	2.06E+06
0.01	7.85E-05	3.14E-02	1.86E-01	3.14E+06	1.30E-01	1.02E-05	9.11E-02	2.29E+06
0.011	9.50E-05	3.46E-02	2.14E-01	2.72E+06	1.37E-01	1.30E-05	1.16E-01	2.51E+06
0.012	1.13E-04	3.77E-02	2.44E-01	2.39E+06	1.43E-01	1.62E-05	1.44E-01	2.74E+06

0.013	1.33E-04	4.08E-02	2.75E-01	2.12E+06	1.49E-01	1.97E-05	1.76E-01	2.97E+06
0.014	1.54E-04	4.40E-02	3.08E-01	1.89E+06	1.54E-01	2.38E-05	2.11E-01	3.20E+06
0.015	1.77E-04	4.71E-02	3.41E-01	1.71E+06	1.60E-01	2.82E-05	2.51E-01	3.43E+06
0.016	2.01E-04	5.03E-02	3.76E-01	1.55E+06	1.65E-01	3.32E-05	2.95E-01	3.66E+06
0.017	2.27E-04	5.34E-02	4.11E-01	1.42E+06	1.70E-01	3.86E-05	3.43E-01	3.89E+06
0.018	2.54E-04	5.65E-02	4.48E-01	1.30E+06	1.75E-01	4.46E-05	3.96E-01	4.12E+06
0.019	2.84E-04	5.97E-02	4.86E-01	1.20E+06	1.80E-01	5.10E-05	4.53E-01	4.34E+06
0.02	3.14E-04	6.28E-02	5.25E-01	1.11E+06	1.85E-01	5.80E-05	5.15E-01	4.57E+06
0.021	3.46E-04	6.60E-02	5.65E-01	1.03E+06	1.89E-01	6.55E-05	5.82E-01	4.80E+06
0.022	3.80E-04	6.91E-02	6.06E-01	9.61E+05	1.94E-01	7.36E-05	6.54E-01	5.03E+06
0.023	4.15E-04	7.23E-02	6.48E-01	8.99E+05	1.98E-01	8.22E-05	7.31E-01	5.26E+06
0.024	4.52E-04	7.54E-02	6.90E-01	8.44E+05	2.02E-01	9.15E-05	8.13E-01	5.49E+06
0.025	4.91E-04	7.85E-02	7.34E-01	7.94E+05	2.06E-01	1.01E-04	9.00E-01	5.72E+06
0.026	5.31E-04	8.17E-02	7.78E-01	7.48E+05	2.10E-01	1.12E-04	9.93E-01	5.94E+06
0.027	5.73E-04	8.48E-02	8.24E-01	7.07E+05	2.14E-01	1.23E-04	1.09E+00	6.17E+06
0.028	6.16E-04	8.80E-02	8.70E-01	6.69E+05	2.18E-01	1.34E-04	1.20E+00	6.40E+06
0.029	6.61E-04	9.11E-02	9.17E-01	6.35E+05	2.22E-01	1.47E-04	1.30E+00	6.63E+06
0.03	7.07E-04	9.42E-02	9.65E-01	6.04E+05	2.26E-01	1.60E-04	1.42E+00	6.86E+06
0.031	7.55E-04	9.74E-02	1.01E+00	5.75E+05	2.30E-01	1.73E-04	1.54E+00	7.09E+06
0.032	8.04E-04	1.01E-01	1.06E+00	5.48E+05	2.33E-01	1.88E-04	1.67E+00	7.32E+06
0.033	8.55E-04	1.04E-01	1.11E+00	5.23E+05	2.37E-01	2.03E-04	1.80E+00	7.54E+06
0.034	9.08E-04	1.07E-01	1.16E+00	5.00E+05	2.41E-01	2.18E-04	1.94E+00	7.77E+06
0.035	9.62E-	1.10E-	1.22E+0	4.79E+05	2.44E-	2.35E-	2.09E+0	8.00E+06

	04	01	0		01	04	0	
0.036	1.02E-03	1.13E-01	1.27E+00	4.59E+05	2.48E-01	2.52E-04	2.24E+00	8.23E+06
0.037	1.08E-03	1.16E-01	1.32E+00	4.41E+05	2.51E-01	2.70E-04	2.40E+00	8.46E+06
0.038	1.13E-03	1.19E-01	1.38E+00	4.23E+05	2.54E-01	2.89E-04	2.56E+00	8.69E+06
0.039	1.19E-03	1.23E-01	1.43E+00	4.07E+05	2.58E-01	3.08E-04	2.74E+00	8.92E+06
0.04	1.26E-03	1.26E-01	1.49E+00	3.92E+05	2.61E-01	3.28E-04	2.92E+00	9.15E+06
0.041	1.32E-03	1.29E-01	1.54E+00	3.78E+05	2.64E-01	3.49E-04	3.10E+00	9.37E+06
0.042	1.39E-03	1.32E-01	1.60E+00	3.64E+05	2.67E-01	3.71E-04	3.29E+00	9.60E+06
0.043	1.45E-03	1.35E-01	1.66E+00	3.52E+05	2.71E-01	3.93E-04	3.49E+00	9.83E+06
0.044	1.52E-03	1.38E-01	1.71E+00	3.40E+05	2.74E-01	4.16E-04	3.70E+00	1.01E+07
0.045	1.59E-03	1.41E-01	1.77E+00	3.29E+05	2.77E-01	4.40E-04	3.91E+00	1.03E+07
0.046	1.66E-03	1.45E-01	1.83E+00	3.18E+05	2.80E-01	4.65E-04	4.14E+00	1.05E+07
0.047	1.73E-03	1.48E-01	1.89E+00	3.08E+05	2.83E-01	4.91E-04	4.36E+00	1.07E+07
0.048	1.81E-03	1.51E-01	1.95E+00	2.98E+05	2.86E-01	5.17E-04	4.60E+00	1.10E+07
0.049	1.89E-03	1.54E-01	2.01E+00	2.89E+05	2.89E-01	5.45E-04	4.84E+00	1.12E+07
0.05	1.96E-03	1.57E-01	2.08E+00	2.81E+05	2.92E-01	5.73E-04	5.09E+00	1.14E+07
0.051	2.04E-03	1.60E-01	2.14E+00	2.72E+05	2.95E-01	6.02E-04	5.35E+00	1.17E+07
0.052	2.12E-03	1.63E-01	2.20E+00	2.65E+05	2.98E-01	6.32E-04	5.62E+00	1.19E+07
0.053	2.21E-03	1.67E-01	2.27E+00	2.57E+05	3.00E-01	6.63E-04	5.89E+00	1.21E+07
0.054	2.29E-03	1.70E-01	2.33E+00	2.50E+05	3.03E-01	6.95E-04	6.17E+00	1.23E+07
0.055	2.38E-03	1.73E-01	2.39E+00	2.43E+05	3.06E-01	7.27E-04	6.46E+00	1.26E+07
0.056	2.46E-03	1.76E-01	2.46E+00	2.37E+05	3.09E-01	7.61E-04	6.76E+00	1.28E+07
0.057	2.55E-03	1.79E-01	2.53E+00	2.30E+05	3.12E-01	7.95E-04	7.07E+00	1.30E+07

0.058	2.64E-03	1.82E-01	2.59E+00	2.25E+05	3.14E-01	8.30E-04	7.38E+00	1.33E+07
0.059	2.73E-03	1.85E-01	2.66E+00	2.19E+05	3.17E-01	8.67E-04	7.70E+00	1.35E+07
0.06	2.83E-03	1.88E-01	2.73E+00	2.13E+05	3.20E-01	9.04E-04	8.03E+00	1.37E+07
0.061	2.92E-03	1.92E-01	2.80E+00	2.08E+05	3.22E-01	9.42E-04	8.37E+00	1.39E+07
0.062	3.02E-03	1.95E-01	2.87E+00	2.03E+05	3.25E-01	9.81E-04	8.72E+00	1.42E+07
0.063	3.12E-03	1.98E-01	2.94E+00	1.98E+05	3.28E-01	1.02E-03	9.08E+00	1.44E+07
0.064	3.22E-03	2.01E-01	3.01E+00	1.94E+05	3.30E-01	1.06E-03	9.44E+00	1.46E+07
0.065	3.32E-03	2.04E-01	3.08E+00	1.89E+05	3.33E-01	1.10E-03	9.81E+00	1.49E+07
0.066	3.42E-03	2.07E-01	3.15E+00	1.85E+05	3.35E-01	1.15E-03	1.02E+01	1.51E+07
0.067	3.53E-03	2.10E-01	3.22E+00	1.81E+05	3.38E-01	1.19E-03	1.06E+01	1.53E+07
0.068	3.63E-03	2.14E-01	3.29E+00	1.77E+05	3.40E-01	1.24E-03	1.10E+01	1.55E+07
0.069	3.74E-03	2.17E-01	3.36E+00	1.73E+05	3.43E-01	1.28E-03	1.14E+01	1.58E+07
0.07	3.85E-03	2.20E-01	3.44E+00	1.69E+05	3.45E-01	1.33E-03	1.18E+01	1.60E+07

Appendix II: Water-walls design:

Based on the number of the phases flowing inside the pipes of the water-walls, the heat transfer analysis is differed. For one-phase flow like in the economizer and the superheater, the heat transfer analysis is shown in page 50. While for two-phase flow like in the boiler, the heat transfer analysis is shown in page 53. For the economizer and the boiler, the outside diameter is in the range of 30 to 80 mm. From ASME/ANSI B36.10 Welded and Seamless Wrought Steel Pipe standard, the outer diameters in this range are shown in the following table. The thickness and the inner diameter are specified using the schedule number, which is:

$$Sch. = 1000\ \frac{P}{S} = 1000\ \frac{(12.5\ MPa)}{(80\ MPa)} = 156$$

Where P is the service pressure and S is the yield strength at 455 C. Since there is no 156 schedule number, schedule 160 is used.

Table 1: outer diameter, thickness and inner diameter for water-walls pipes

Outer diameter (m)	Thickness (m)	Inside diameter (m)
0.0334	0.00635	0.0207
0.0422	0.00635	0.0295
0.0483	0.00714	0.03402
0.0603	0.00874	0.04282
0.073	0.00953	0.05394

To know the number of pipes, length, and optimal diameter, the amount of heat that needs to be added must be known. The amount of heat accepted by the cold flow (flow inside the pipe) is the same as the amount of heat transferred from the hot flow. The table below shows the amount of heat needed for the two sets of water-walls. For the non-pressurized water-walls, there is no need for an economizer because the flow comes from the turbine as a saturated mixture.

Table 2: Heat requirement for pressurized and non-pressurized water-walls.

Type		Q (MW)
Pressurized	Economizer	266
	Boiler	125.2
	Superheater	39.4
Non-pressurized	Boiler	31.26
	Superheater	54.8

Sample Calculation: Pressurized economizer

The economizer is used to perform a sample calculation with an outside diameter being 0.0334m and inside diameter being 0.0207m. From the analysis in page 50, the following equations are used to find the optimal length and number of pipes:

$$\frac{q}{L} = n\left(\frac{U_o A_o}{L}\right)\Delta T_{lm}$$

$$\Delta T_{lm} = \frac{\Delta T_o - \Delta T_i}{\ln\left({}^{\Delta T_o}/_{\Delta T_i}\right)} = 244\ K$$

$$\Delta T_o = T_{\infty,o} - T_o = 455 - 327 = 128\ K$$

$$\Delta T_i = T_{\infty,o} - T_i = 455 - 40 = 415\ K$$

where $T_{\infty,o}$ is the temperature of the bed (heating temperature)

T_o is the outlet temperature (i.e. saturated liquid temperature for the economizer)

T_i is the inlet temperature (i.e. saturated vapor temperature for the superheater)

$$\left(\frac{UA}{L}\right) = \frac{1}{\frac{1}{2\pi r_o h_o} + \frac{\ln\left({}^{r_o}/_{r_i}\right)}{2\pi k} + \frac{1}{2\pi r_i h_i}}$$

where r_o is outside radius r_i is the inside radius

h_o is the outside convective heat transfer coefficient = 400 W/m^2-K

h_i is the inside convective heat transfer coefficient

k is thermal conductivity of the walls material= 32.9 W/m-K

$$h_i = \frac{Nu_D D}{k} = \frac{0.023\ Re^{4/5} Pr^{0.4}\ D}{k}$$

$$Re = \frac{4\ (\frac{\dot{m}}{n})}{\pi D \mu}$$

Where Nu_D: Nussult number D: inside diameter

k: thermal conductivity Re: Reynolds's number

Pr: Prandtl number= 1.72 $\dot{m}$: mass flow rate =129.9 kg/s

n: number of pipes μ: dynamic viscosity= 207.1x 10^{-6} Pa-s

Applying these equations, the length of each pipe is a function of the number of pipes. The table below shows the length of the number of the water-walls pipes and the corresponding length and volume of the thickness. Volume of the thickness is calculated be multiplying the area of the pipe thickness by the length of each pipe by the number of pipes. The smaller the volume of the thickness, the less amount of material is used which leads to a lower cost. The criterion for optimization is based on the spacing (S) between the pipes and it is set to be at least one diameter (D) long. That is, the maximum D/S= 100%. Therefore, values over 100% are neglected in the table. From the table, the optimum number of pipes is 330 and the corresponding length is 17.93m.

Table 3: Pressurized economizer with an outer diameter= 0.0334 m, and inside diameter= 0.0207m.

n	L (m)	V (m^3)	D/S
10	1512.85	8.16	2.95
20	594.93	6.42	5.91
30	351.12	5.68	8.86
40	243.07	5.25	11.81
50	183.28	4.95	14.77
60	145.77	4.72	17.72
70	120.23	4.54	20.67
80	101.83	4.40	23.63
90	87.99	4.27	26.58
100	77.24	4.17	29.53
110	68.66	4.08	32.49
120	61.68	3.99	35.44

130	55.90	3.92	38.39
140	51.04	3.86	41.34
150	46.90	3.80	44.30
160	43.33	3.74	47.25
170	40.23	3.69	50.20
180	37.51	3.64	53.16
190	35.12	3.60	56.11
200	32.98	3.56	59.06
210	31.08	3.52	62.02
220	29.36	3.49	64.97
230	27.81	3.45	67.92
240	26.41	3.42	70.88
250	25.13	3.39	73.83
260	23.96	3.36	76.78
270	22.88	3.33	79.74
280	21.89	3.31	82.69
290	20.98	3.28	85.64
300	20.13	3.26	88.60
310	19.34	3.24	91.55
320	18.61	3.21	94.50
330	17.93	3.19	97.46
340	17.29	3.17	100.41
350	16.69	3.15	103.36
360	16.13	3.13	106.32
370	15.61	3.12	109.27
380	15.11	3.10	112.22

As can be seen from the table above, the optimal number of pipes is 330 and the corresponding length and volume of thickness are 17.93 m and 3.19 m^3. The same method is applied to the other diameters and the optimal values are shown in the following table.

The optimal number of pipes from each diameter set is shown below for the economizer

Table 4: Optimal number of pipes for the economizer for each diameter.

OD (m)	t (m)	ID(m)	n	L(m)	V (m^3)
0.0334	0.00635	0.0207	330	17.93	3.19
0.0422	0.00635	0.0295	260	15.10	2.81
0.0483	0.00714	0.03402	230	15.42	3.27
0.0603	0.00874	0.04282	180	15.84	4.03
0.073	0.00953	0.05394	150	15.1	4.3

As can be seen, the 0.0422 m outer diameter has the smallest thickness volume, which makes it the optimal diameter for the economizer.

For the superheater the same method is followed, but the diameter of pipes ranges from 50 mm to 80 mm. The table below shows the optimal diameter for the pressurized and non-pressurized water-walls in the superheater.

Table 5: optimal number of pipes for the pressurized and non-pressurized superheater for each diameter.

Type	OD (m)	t (m)	ID (m)	n	L (m)	V (m^3)
Pressurized	0.0603	0.00874	0.04282	180	6.35	1.62
	0.073	0.00953	0.05394	150	6.82	1.80
Non-Pressurized	0.0603	0.00874	0.04282	150	10.07	2.13
	0.073	0.00953	0.05394	150	7.66	2.18

Sample Calculations for the boilers:

As shown in section 5.3.2.2, UA/L equation reduces to

$$\left(\frac{UA}{L}\right) = \frac{1}{\frac{1}{2\pi r_o h_o} + \frac{\ln\left({}^{r_o}/_{r_i}\right)}{2\pi k}}$$

While the temperature difference between the hot bed and the inside flow is:

$$\Delta T = T_{\infty,o} - T_o$$

For example, the temperature difference in the non-pressurized boiler pipes is 455-100= 355 K. And since,

$$q = \frac{\Delta T}{R}$$

Therefore,

$$R = \frac{\Delta T}{q} = \frac{355\ (K)}{31.26\ (MW)} = 1.135 * 10^{-5}\ (K/W)$$

Since the water-walls extend from the water drum to the steam drum, the economizer and the boiler have the same pipe diameter. Therefore, it is assumed that the boiler in the pressurized and non-pressurized water-walls will have the same pipe diameter (D_o= 0.0422 m) and the same number of pipes (260).

$$R = \frac{1}{n\,L}\left[\frac{\ln\left({}^{r_o}/_{r_i}\right)}{2\pi k} + \frac{1}{2\pi r_o h_o}\right] = \frac{1}{L}[\ 0.0205]$$

Resulting in the length of each pipe being 6.94 m. Table below summarizes the optimal number of pipes, and the corresponding length and volume of thickness for the pressurized and non-pressurized water-walls.

Table 6: Water-walls optimal diameter, length and volume.

Type		Q (MW)	Optimal diameter (m)	Number of pipes	Length of pipes (m)	Thickness volume (m^3)
Pressurized	Economizer	266	0.0422	260	15.10	2.81
	Boiler	125.2	0.0422	260	7.7	1.43
	Superheater	39.4	0.0603	180	6.35	1.62
Non-pressurized	Boiler	31.26	0.0422	260	6.94	1.29
	Superheater	54.8	0.0603	150	10.07	2.13

References:

Abedin, Ali Haji. *Thermochemical Energy Storage Systems: Modelling, Analysis and Design*. Thesis. University of Ontario Institute of Technology, 2010.

"ASTM A53/106 GR. A/B carbon seamless steel pipe" Alibaba, n.d. Web. 13 Apr. 2016. < http://www.alibaba.com/product-detail/ASTM-A53-106-GR-A-B_428915350.html?spm=a2700.7724838.0.0.JCNwci&s=p>.

Barker, Ronald. "The Reversibility of the Reaction CaCO3↔CaO+CO2." *Journal of Chemical Technology and Biotechnology* 23.10 (1973): 733-42. Web.

Basu, Prabir. *Circulating Fluidized Bed Boilers: Design, Operation and Maintenance*. Cham: Springer, 2015. Print.

Brigham, B. A., and G. J. VanFossen. "Length to Diameter Ratio and Row Number Effects in Short Pin Fin Heat Transfer." *Journal of Engineering for Gas Turbines and Power* 106.1 (1984): 241-44. Web.

Bogdanović, B., B. Spliethoff, Active MgH2Mg-systems for hydrogen storage, International Journal of Hydrogen Energy, Volume 12, Issue 12, 1987, Pages 863-873

"C1100 Copper Rod Price." Alibaba, n.d. Web. 13 Apr. 2016. <http://www.alibaba.com/product-detail/Hot-Sale-C1100-Copper-Rod-Price_60064473575.html?spm=a2700.7724838.30.1.WJEgB2>.

Cekirge, Huseyin Murat, and Elhassan, Ammar. A Comparison of Solar Power Systems (CSP): Solar Tower (ST) Systems versus Parabolic Trough (PT) Systems. American Journal of Energy Engineering. Vol. 3, No. 3, 2015, pp. 29-36

Chase, Malcolm W. J. *NIST-JANAF Thermochemical Tables, 4th Edition*. Tech.1998.

Çengel, Yunus A., and Michael A. Boles. *Thermodynamics: An Engineering Approach*. New York, NY: McGraw-Hill, 2011. Print.

Criado, Yolanda A., Mónica Alonso, and J. Carlos Abanades. "Kinetics of the CaO/Ca(OH)2 Hydration/Dehydration Reaction for Thermochemical Energy Storage Applications." *Industrial & Engineering Chemistry Research* 53.32 (2014): 12594-2601. Web.

Felderhoff, M., R. Urbanczyk, and S. Peil. "Thermochemical Heat Storage for High Temperature Applications – A Review." *Green* 3.2 (2013): 113-23. Web.

Gil, Antoni, Marc Medrano, Ingrid Martorell, Ana Lázaro, Pablo Dolado, Belén Zalba, Luisa F. Cabeza, State of the art on high temperature thermal energy storage for power generation. Part 1—Concepts, materials and modellization, Renewable and Sustainable Energy Reviews, Volume 14, Issue 1, January 2010, Pages 31-55

Grace, John R., A. A. Avidan, and T. M. Knowlton. *Circulating Fluidized Beds*. London: Blackie Academic & Professional, 1997. Print.

"High quality manufacturer powder calcium hydroxide price" Alibaba, n.d. Web. 13 Apr. 2016. <http://www.alibaba.com/product-detail/2015-high-quality-manufacturer-powder-calcium_60189694093.html?spm=a2700.7724857.29.27.gDBXD4>.

Incropera, Frank P. *Introduction to Heat Transfer*. Hobokenm NJ: Wiley, 2007.

MacKay, David J. C. Sustainable Energy--without the Hot Air. Cambridge, England:UIT, 2009. Print.

Palmer, Karen, Richard Sweeney, and Maura Allaire. *Modeling Policies to Promote Renewable and Low-Carbon Sources of Electricity*. Rep. N.p.: NEPI, 2010. Print.

Pardo, P., A. Deydier, Z. Anxionnaz-Minvielle, S. Rougé, M. Cabassud, P. Cognet, A review on high temperature thermochemical heat energy storage, Renewable and Sustainable Energy Reviews, Volume 32, April 2014, Pages 591-610

Rosemary, J. K.; Bauerle, G. L.; Springer, T. H. Solar energy storage using reversible hydration/dehydration of CaO-Ca(OH)2, AIAA Terrestrial Energy Systems Conference, Orlando, Florida, 1979; 79-0986.

Spencer, H.M. *Ind. Eng. Chem.,* vol 40, pp. 2152-2154, 1948.

Teir, Sebastian. "Thermal Design of Heat Exchangers." *Steam Boiler Technology*. Espoo: Helsinki U of Technology, 2003. N. pag. Print.

Tempkin, M.J, and V. Pyzhev, "Kinetics of Ammonia Synthesis on Promoted Iron Catalysts," Acta Physiochim, URSS, Vol. 12, 1940, pp. 217-222.

Twidell, John, and Anthony D. Weir. Renewable Energy Resources. London: Taylor & Francis, 2006. Print.

Tyner, C., D. Wasyluk, eSolar's Modular, Scalable Molten Salt Power Tower Reference Plant Design, Energy Procedia, Volume 49, 2014, Pages 1563-1572

United Nations, Department of Economic and Social Affairs, Population Division (2015). *World Population Prospects: The 2015 Revision, Key Findings and Advance Tables*. Working Paper No. ESA/P/WP.241.

"Updated Capital Cost Estimates for Utility Scale Electricity Generating Plants" *U.S. Energy Information Administration - EIA - Independent Statistics and Analysis*. 12 Apr. 2013.

Welded and Seamless Wrought Steel Pipe. Tech. Vol. B36.10. New York: ASME, 2004. Print.

Wentworth, W.E., E. Chen, Simple thermal decomposition reactions for storage of solar thermal energy, Solar Energy, Volume 18, Issue 3, 1976, Pages 205-214
What Is AGC Plibrico: Refractory specifications. Apr. 2013. Web. 1 Apr. 2016. <http://www.plibrico.co.jp/Portals/0/images-en/products/products/AGC_Plibrico.pdf>.

“What is U.S. electricity generation by energy source?" U.S. Energy Information Administration - EIA - Independent Statistics and Analysis. 2015.

Woodruff, Everett B., Herbert B. Lammers, and Thomas F. Lammers. *Steam Plant Operation*. New York: McGraw-Hill, 2005. Print.